THE ANALYSIS AND IMPROVEMENT OF A 1.2 METER CURVED CRYSTAL SPECTROMETER AND ITS APPLICATION TO THE MEASUREMENT OF RELATIVE INTENSITIES OF IRIDIUM-192 GAMMA RAYS

A Thesis

Presented to

the Faculty of Graduate Studies

The University of Manitoba

In Partial Fulfillment

of the Requirements for the Degree

Master of Science

by

Mahadeva Chakraborty

October 1965

UNIVERSITY OF MANITOBA ELIZABETH DAFOE LIBRARY

PREFACE

The work presented in this thesis was carried out at the University of Manitoba during October, 1964 - April, 1965.

The author wishes to express his gratitude to Dr. D. G. Douglas for his valuable advice and supervision of the thesis project.

The financial assistance provided by the Physics Department, University of Manitoba is gratefully acknowledged.

The author also wishes to acknowledge the help rendered to him in various ways by his friends at the Physics Department, University of Manitoba and at the Physics Department, Manitoba Cancer Treatment and Research Foundation.

ABSTRACT

Work described in this thesis is mainly divided into two parts: (1) Performance analysis of a 1.2 meter curved crystal spectrometer. (2) Determination of the relative intensities of Iridium - 192 gamma rays.

Performance of the curved crystal was analysed by scanning it part by part, as it was suspected that the crystal had not been properly bent. Result of this analysis showed that, be deleting certain portions of the curved diffraction crystal better shaped line profiles could be obtained and resolution of the instrument could be improved. 37% of the crystal aperture was deleted. This, however, did not affect the counting rate to any considerable amount.

Relative intensities of 13 gamma transitions of Ir - 192 have been determined, most of which agree fairly well with values reported by other research workers (who have determined these values either by crystal diffraction method or by photo conversion method). Relative intensities for the 283, 375, and 416.6 kev lines have been determined. This has not been done earlier by crystal diffraction method. Relative intensities for these lines are 3.4, 8, and 10 respectively.

An empirical efficiency rule for the curved crystal diffraction spectrometer operated in tandem with the scintillation spectrometer as one unit, has been determined experimentally. This rule is quoted here. Relative intensity (R.I.) = const. x Photopeak area (Ap) x $E^{3.453}$, where E is the gamma energy.

The reflection coefficient, R, of 310 quartz plane has been determined as $R = \text{const.}\ E^{-1.95}$, where E is the gamma energy.

This is in fair agreement with values given by other workers. R was determined in the following way. For each line, relative intensity

not corrected for the reflectivity of the crystal was divided by the respective relative intensity value obtained from the efficiency rule. These ratios were plotted against reciprocals of respective gamma energies on a log-log graph paper. The line passing through these points was a straight line. From the slope of this straight line, the above value for R. was determined.

Energy resolution as a function of energy, for the curved crystal diffraction spectrometer, has been determined.

TABLE OF CONTENTS

	PAGE
PREFACE	
ABSTRACT	
CHAPTER I	
GENERAL INTRODUCTION	1
CHAPTER II	
INTRODUCTION TO THE PRESENT INSTRUMENT	4
The clamping blocks and the crystal	8
The baffle system	9
The radiation detector	9
The source holder	11
CHAPTER III	
HARTMANN TEST	12
Introduction	12
Experimental procedure	12
Experimental observations	15
Improvement of the aperture	19
Discussion	20
Optical test	26
CHAPTER IV	
RELATIVE INTENSITY MEASUREMENT OF IRRIDIUM-192 GAMMA RAYS	31
Introduction	31
The source	32
Procedure (experimental)	34

Procedure (analytical) 35

Analysed data 38

Discussion 39

Determination of efficiency rule 41

Conclusion 43

CHAPTER V

Determination of the reflection coefficient of the present crystal 44

Determination of the energy resolution of the diffraction spectrometer 44

Search for other lines 45

APPENDIX

LIST OF REFERENCES

INDEX FOR TABLES, PLATES AND FIGURES

TABLE	NEXT TO PAGE
I	14
II	18
III	19
IV	39
V	34
VI	35
VII	38
VIII	41
IX	42
X	44

PLATE	NEXT TO PAGE
1	5
2	12
3	13
4 A and B	18

FIGURE	NEXT TO PAGE
A and B	2
1	4
2	5
3	11
4	13
5	14
6	14
7	14
8	15
9	17
10	18
11	19
12	19
13, 14 and 15	20
16	25
17	25
18	26
19	27
20	27
21	35
22	35
23	41
24	43
25	44

CHAPTER I

GENERAL INTRODUCTION

The subject of crystal diffraction spectroscopy concerns diffraction of x-rays and gamma rays from single crystals, and determination of their energies and intensities from the angular distribution of these rays. For any useful information, the rays, which are scattered elastically (i.e. without loss of energy) by the average spatial distribution of electrons surrounding each atom (of the crystal lattice) are of interest.

The wavelength (from which energy can be calculated) of the radiation under study is given by the well known Bragg equation

$$n \lambda = 2 d \sin \theta_B.$$

Here n is the order of diffraction, λ is the wavelength of radiation, d is the interplane spacing (which is constant for a particular crystal plane) and θ_B is the Bragg diffraction angle, which corresponds to the direction of maximum intensity of the diffracted ray (i.e. the radiation under study).

If the diffraction planes are perpendicular to the incident and exit surfaces of a crystal lamina, then, for rays transmitted and diffracted by the crystal lamina, the refraction at the crystal surface is such that this Bragg equation holds for both internal and external wavelengths and diffraction angles. So, correction to the observed Bragg angle for the refractive index of the crystal used is not necessary.

Most of the crystal spectrometers used for x-ray and gamma ray study are of the transmission type and the crystal laminae used in such

spectrometers are cut with the diffracting planes perpendicular to their incident and exit surfaces.

The study of nuclear gamma rays by direct crystalline diffraction method was first made by Rutherford and Andrade[1]. This was reported in the year 1914. They could measure gamma rays of energy up to 177 kev, (70 mÅ). Another arrangement, the rotating crystal technique of Bragg[2], was used first by Thibaud[3] (in 1925) and then by Frilley[4] (in 1929) for the study of nuclear gamma rays. Frilley could measure gamma rays of energy up to 774 kev (16 mÅ).

These early attempts are of historical importance only. The precision was poor and the resolution was low. Moreover, the measurements at small diffraction angles were obscured by relatively intense background due to direct and diffusely scattered radiation.

In 1930, DuMond[5] suggested a curved crystal focussing x-ray spectrometer technique. This was first practically realised by Cauchois[6] (1932). In 1934, she recorded, photographically, x-rays emitted by extended sources of different radioactive isotopes following diffraction from a curved crystal. The shortest wavelengths measured with this arrangement were about 160 mÅ[7]. Here again the chief difficulty in reaching the shorter wavelength domain was that of shielding the film from the directly transmitted gamma ray beam so that it might not obscure the spectrum of selectively reflected lines.

A major advance in the measurement of nuclear gamma rays by crystal diffraction was made in 1947[8] with the development of DuMond's 2 metre curved crystal spectrometer. His spectrometer is really a monochromator of variable wavelength rather than a spectrograph since with it the intensity of only one wavelength at a time can be observed at each angular setting. The source is moved to successive wavelength positions on the

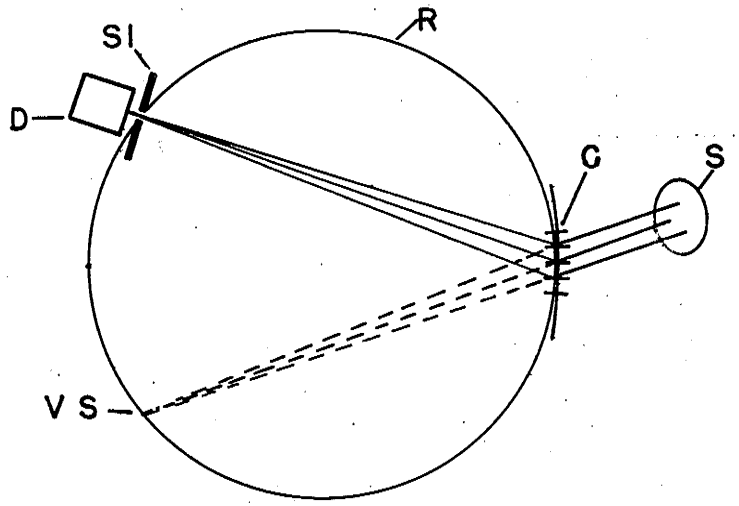

Fig. A.

The Cauchois arrangement of a curved crystal transmission spectrometer.

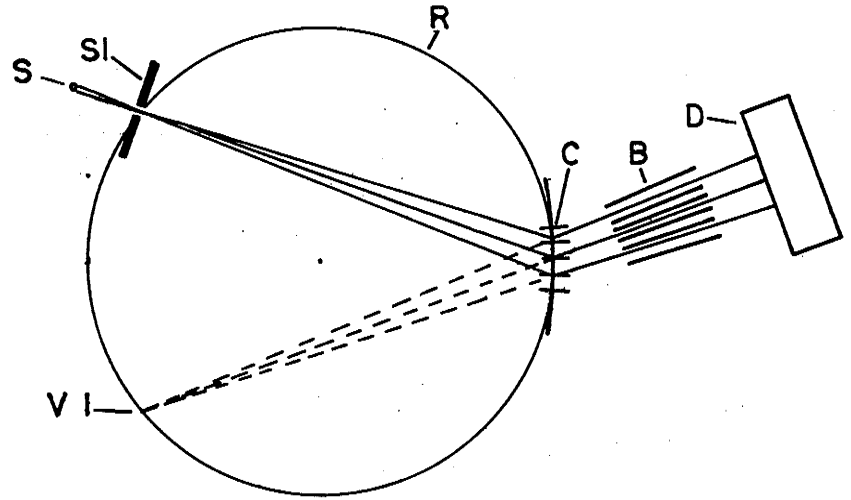

Fig. B.

The DuMond arrangement of a curved crystal transmission spectrometer.

CHAPTER II

INTRODUCTION TO THE PRESENT INSTRUMENT

The instrument, used for work described in this thesis (i.e. the present instrument), was constructed in this precision gamma-ray spectroscopy laboratory a few years ago, under the supervision of Dr. D. G. Douglas. It is essentially a DuMond type curved crystal (1.24 metres in radius) transmission gamma-ray spectrometer. Mr. John F.Moore was the first student to use it. Details of its construction and working have been reported by him in his M. Sc. thesis dated October, 1959. Its basic features are briefly reviewed here.

A quartz crystal lamina (about a millimeter in thickness) is elastically bent to form part of a right circular cylinder of radius 1.24 meters by applying force normal to the surface of the crystal lamina with the help of two clamping blocks. The transverse crystal planes, normal to the crystal surface, therefore converge to a line coinciding with the axis of the cylinder. The radioactive line source is kept parallel to this axis. The source is constrained to move on the surface of a right circular cylinder whose axis is parallel to the axis of the cylindrically bent crystal. The diameter of this right circular cylinder is equal to the radius of curvature of the bent crystal. This right circular cylinder (on which the source moves) passes through the axis of the bent crystal, touching the crystal tangentially.

For discussing the operation of the spectrometer, it is convenient to consider a cross section normal to the axes of these cylinders. Thus, let the crystal be considered as the arc of a circle and the source as

Figure 1.

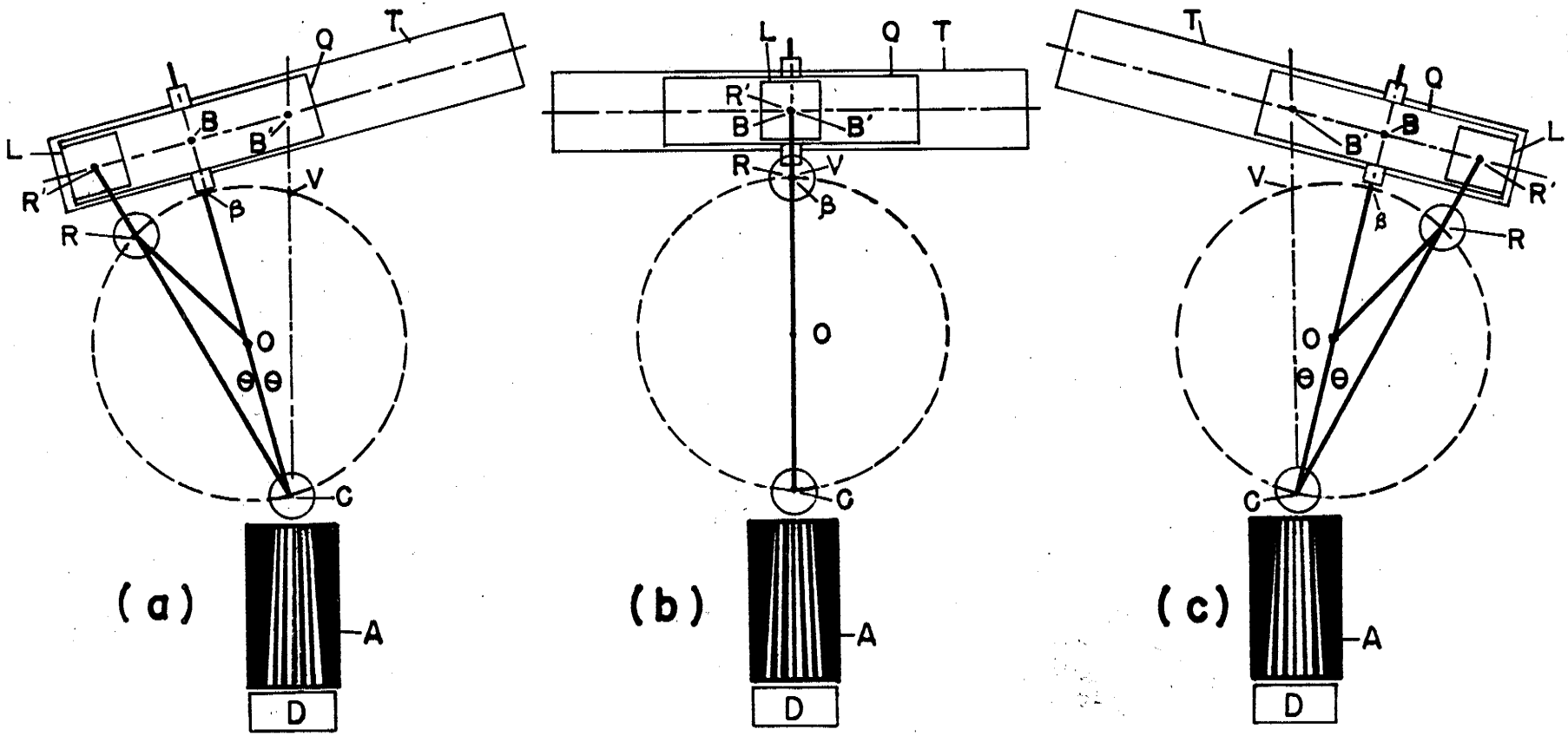

FIGURE 1. Schematic illustration of the geometry of the curved crystal gamma-ray spectrometer. The view at center shows the instrument at the zero wavelength position. The views (c) and (a) show different wavelength settings for reflections to left and to right of the atomic reflecting planes. The drawing is not to scale. For explanation, see page 5 of the text.

a point moving on a circle of diameter equal to the radius of the circle to which the crystal has been bent. The smaller circle, called the focal circle (or the Rowland circle) passes through the centre of the circle to which the crystal has been bent and through the centre, C of the crystal itself.

The directions of the selectively reflected rays from transverse atomic planes of the quartz crystal are kept fixed so that these rays can pass through the Soller slit system (or baffle collimator) reaching the detector at its other end, both the collimator and the detector are kept fixed in space. To accomplish this, the crystal is rotated, (and consequently the focal circle), about its central axis by half the angle of rotation of the source (which is constrained to move on the focal circle) around this central axis of the crystal. Figure 1 illustrates schematically the geometry of the spectrometer.

The same reference letters apply to figures 1 and 2. The big circle CVR is the focal circle. C - centre of the crystal, R - source position, V-virtual image position, β - zero of the wave length scale, O - centre of the focal circle, A - baffle collimator, D - detector, CB - length of the lower radial beam which is always perpendicular to the tangent to the crystal surface at C, CR' - length of the upper radial beam which carries the source, L - upper carriage, Q - lower carriage, T- the track, and B' - centre of the track. CB is perpendicular bisector of the line R'B'. CV joins B', if extended.

In figure 1, the view at centre shows the instrument at the zero wavelength position, while the views to left and right show different wavelength settings for reflections to left and to right of the atomic reflecting planes. Here the line joining the source with point C (through which the central axis of the crystal passes) rotates at twice the rate

FIGURE 2.

PERSPECTIVE LINE DRAWING OF THE CURVED CRYSTAL GAMMA RAY SPECTROMETER. (Not to scale.)
For explanation, see page 6 of the text.

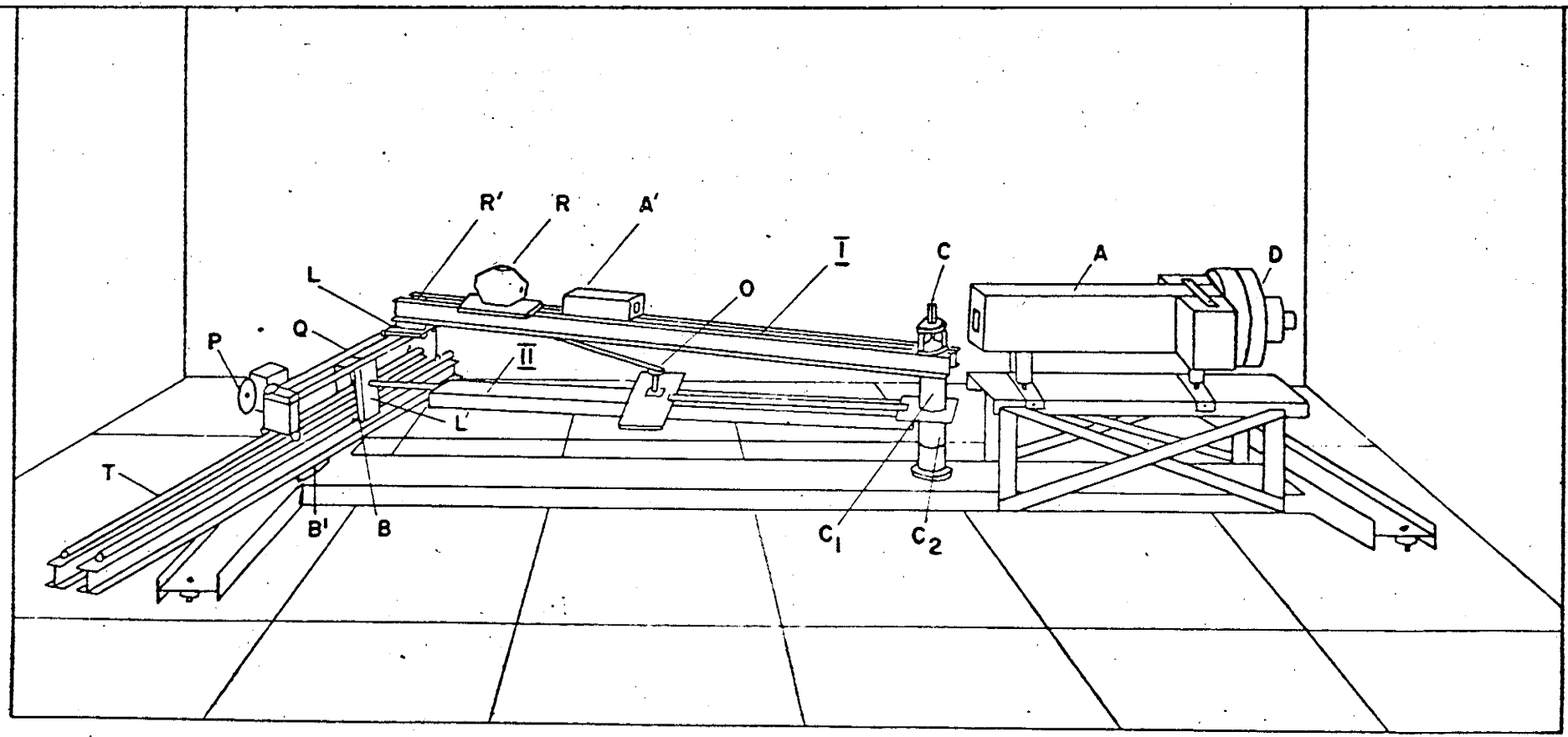

5a

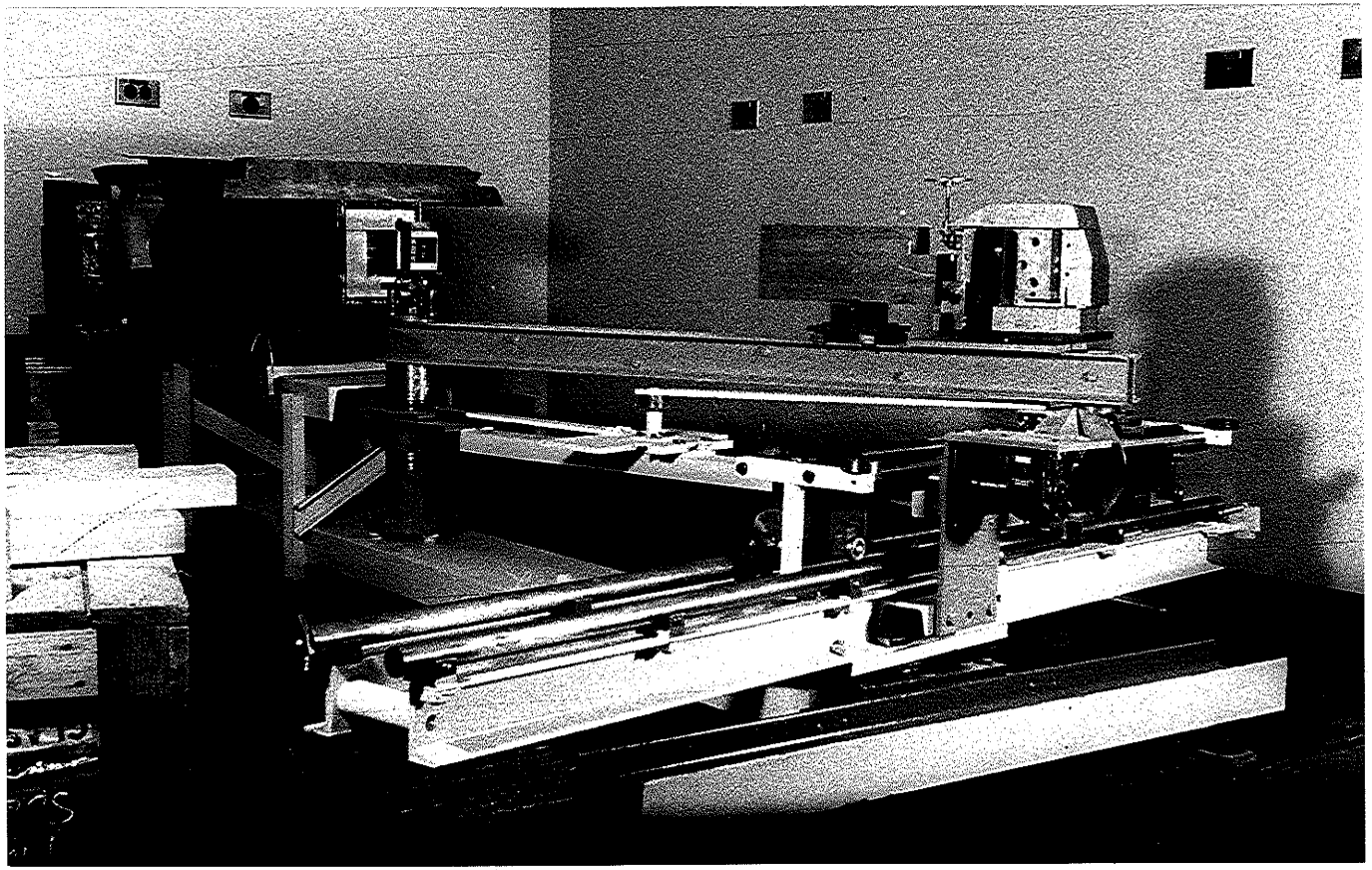

PLATE 1

Over-all view of the 1.2 meter curved crystal spectrometer.
(Source position is on the RIGHT side.)

with which the crystal rotates. The virtual image point V then remains in a fixed position directly opposite to the baffle collimator or Soller slit system A.

The ability to study the spectra resulting from reflection on either side of the transverse atomic reflecting planes as pointed out above, removes the need for knowing beforehand the exact position of β, the zero of the wavelength scale.

Actual working of the instrument can be followed from figure 2.

O defines the centre of focal circle whose diameter is 1.24 metres. The radius bar OR of the focal circle joins the source carriage R, on the upper radial beam CR' to the pivot O, supported on the lower radial beam. The upper radial beam I, constructed of two channel sections held apart by spacers and pivoted at C, is capable of swinging, independently of the crystal holder and lower radial beam II and in a horizontal arc about the point C. The source carriage, which rides on this upper beam on steel ball bearing ways, can travel a short distance along the beam's length, as dictated by the motion of the radius bar. (This is necessary to keep the source on the focal circle.)

The small collimator A', placed on the upper radial beam directly in front of the source carriage, acts as a guiding device for the radiation incident on the crystal. The lower beam, also pivoted at C, at a lower height (being fixed to the cylindrical steel bearing C_2) and capable of swinging in a horizontal arc, is rigidly clamped to the crystal holder by means of a vertical shaft which passes down through the cylindrical steel bearing (C_1) for the upper beam.

The unpivoted end of the lower radial beam terminates in a length of cylindrical steel shafting which rides on roller bearings through a

support L' in carriage Q. This makes the distance CB capable of variation (figure 1).

The small carriage L, on which the unpivoted end of the upper radial beam rests, is free to move on two cylindrical steel roller bearings (held apart by spacers) on the lower carriage Q, which, in turn, is free to move on the track T. The track T can rotate in a horizontal plane about a cylindrical steel spindle B' fixed to the base of the instrument. The unpivoted end of the lower radial beam is fixed to the carriage, Q. To drive the spectrometer, a spur gear is held fixed on a steel plate mounted rigidly on a steel upright attached to the track T, at its middle, where it passes through the steel spindle B'. This spur gear engages a steel saw tooth rack fixed to the lower carriage Q. This rack and pinion system allows the carriage to be driven along the track by the turning of a circular brass disc P which is geared down in a ratio of fifty to one. As the lower carriage Q is driven along the track, the upper carriage L, and consequently the end of the upper radial beam (on which the source carriage lies), is constrained by means of a pulley system to move along the lower carriage (to which the lower radial beam is fixed) in the same direction but at twice the rate. (As the crystal holder is rigidly clamped to the other end of the lower radial beam, this means that the source rotates by twice the angle of rotation of the crystal around the axis through C.)

The whole instrument is supported upon a heavy channel base which can be levelled by means of six heavy screws. The baffle, or Soller slit system A and detector head D are placed beyond the curved crystal at a proper elevation.

Wavelength measured by the curved crystal spectrometer is propor-

tional to the sine of the angle θ at which the gamma radiation is incident on the transverse planes of the curved crystal. From figure 1, it can be observed that R'BC is a right angled triangle with a constant hypotenuse R'C. So the wavelength is proportional to the length R'B, which corresponds to the distance of travel of the spur gear along the rack from the "zero" position. This is measured by means of the brass disc (dial) P geared to the rack and pinion assembly. The number of complete revolutions of this brass disc is given by a small revolution counter fixed to its axle. The brass disc can directly give readings up to 1/10 of its revolution.

Calculation for the distance R'B is shown here.

0.6π inches is the diameter of the spur gear. The spur gear turns at 50:1 ratio of the dial, so travel per turn of the spur gear on the saw tooth rack is $(1/50) \times 0.6\pi = 0.0377$ inches. Therefore the distance R'B is 0.0377n, where n is the total number of turns of the dial.

The constant distance R'C is 51.991 ± 0.005 inches. From these data, Sin θ and so, the wavelength can easily be calculated. (For very small angles, as a first approximation, sin θ can be taken as equal to the angle θ itself.)

The full width at half maximum for each energy line profiles in seconds of arc ($\delta\theta$) can easily be calculated from a knowledge of the width in dial reading (δD). They are related as follows:

$$\delta\theta = 150.8 \times \delta D \text{ seconds.}$$

Derivation of the relation is shown in the Appendix.

<u>The clamping blocks and the crystal</u>.

The diffracting quartz crystal is held between two specially machined stainless steel clamping blocks C . These blocks are machined into a

matching convex-concave set, the radius of curvature being the radius to which the crystal is bent. A rubber gasket separates the crystal slab from the concave block. The two blocks are held together by four bolts fitted with helical springs. Pressure is applied by springs rather than by the bolts directly, to allow for any small contractions or expansions due to temperature changes. This clamping block assembly is clamped onto a table which is rigidly fixed, by means of a vertical shaft, through the cylindrical steel bearing C_1, to the lower radial beam as described earlier.

The convex block has a ribbed window of dimensions about 5.8 cm. by 4.8 cm., which determines the aperture of the crystal. The purpose of the ribs is to supply the centre of the crystal with support and to ensure an accurately curved profile.

The transverse reflecting planes of the quartz crystal (which are perpendicular to its surface) are the 310 planes which have a grating distance 'd' of 1.1776 Å. Thickness of the crystal lamina is about 1 mm.

The baffle system.

The baffle or Soller slit system A (figure 2 and plate 1) consists of fifty slots and fifty babbitt fins each of width 0.040 inches at one end (nearer to the detector) and 0.025 inches at the other end (nearer to the diffracting crystal). They have been tapered to converge at the source when the Bragg angle is zero. The purpose of the baffle system is to shield the detector from the direct radiation beam at Bragg angles different from zero, and to transmit only the properly diffracted rays.

The radiation detector.

A NaI (Tl) crystal, $4\frac{1}{2}$ inches in diameter and $\frac{1}{2}$ inch thick, is used as the detector for the diffracted gamma rays. The large diameter is necessary for receiving all of the diffracted rays transmitted through

the Soller slit system, whereas, the smaller thickness is useful in keeping the background counts due to stray radiations (other than from the source) low. The crystal is encased in a thin aluminum covering to protect it from moisture. A phototube mounted on the back surface of the crystal is connected to an electronic counting circuit. The phototube and crystal assembly is made light-tight. This scintillation crystal is surrounded by a thick iron ring so as to reduce the background due to any radioactive material present in the lead shielding. This crystal and phototube assembly is mounted on the baffle collimator at the diverging end of the babbitt fins.

The pulses from the phototube are passed through a preamplifier to a Franklin amplifier. The output of the amplifier is passed through a pulse height selector to a scaler. The pulse height selector enables the pulses produced by gamma ray photons of one energy to be counted.

Thus, the system used to detect the selectively reflected gamma rays is essentially a scintillation spectrometer operated in tandem with the curved crystal spectrometer.

As the spectrum is scanned by the curved crystal spectrometer (which is really a monochromator of variable wavelength), the differential bias level in the scintillation spectrometer is varied so that the pulse height selector gate admits only pulses having the same energy as the gamma rays reflected according to the Bragg relation by the curved crystal. In this manner, a large fraction of the background pulses due to cosmic rays and scattered gamma rays are removed from the spectrum.

As a check against backlash, the radial beams of the curved crystal spectrometer is driven in only one direction along the tracks from the be-

ginning to the end of the spectral line profile.

The source holder.

The radio-active source is held in an aluminum vice which is mounted in a babbitt block, which in turn is placed inside the source castle R (figure 2 and plate 1). This arrangement attenuates the radiation from the source to a biologically safe limit. A narrow slit in the castle allows a sharp beam of gamma radiation to strike the quartz crystal.

The source castle R is mounted on the source carriage. This mounting is such that, the source slit (which is in the front of the source castle) is always on the focal circle.

FIGURE 3.

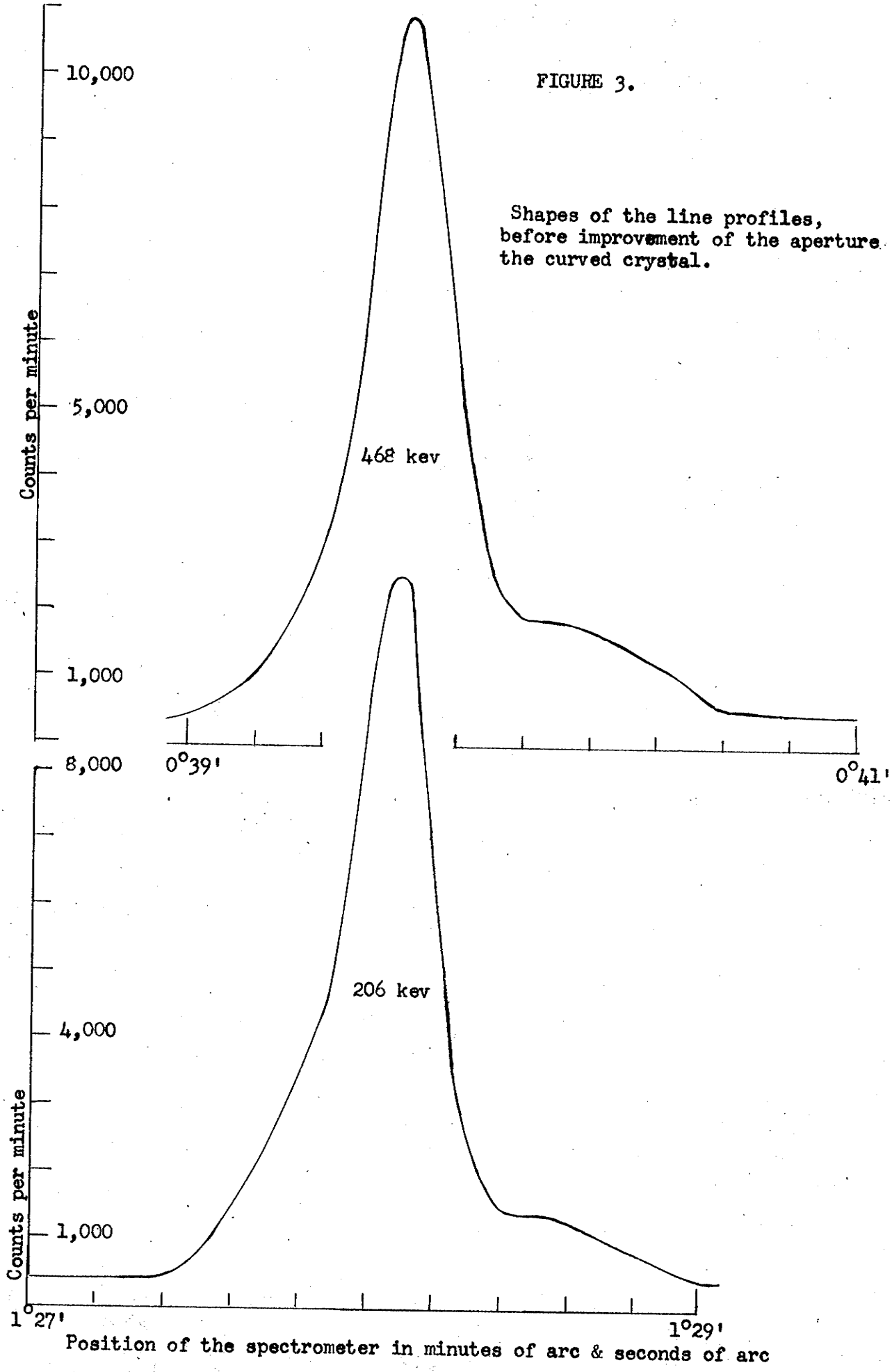

Shapes of the line profiles, before improvement of the aperture of the curved crystal.

CHAPTER III

HARTMANN TEST

Introduction:

The name Hartmann test has been drawn from analogy with the well-known Hartmann method of testing the aberrations of focus of large astronomical mirrors. In this test a small fraction of the whole aperture is studied at a time. Need for such a test for the present curved (cylindrically bent) crystal was felt necessary after observing that the spectral line profiles for different gamma energies of Iridium-192 were far from symmetrical in shape.

The line profiles for different energies actually showed the following features:

(1) Higher energy side of each line profile was steeper compared to its counter part on the lower energy side, i.e. the profile rose more as a slanting line than as a smooth curve.

(2) Lower energy side of every spectral line had a small hump at its tailing end. Also it had a longer tail compared to its counter part of the higher energy side.

These features of the line profiles have been illustrated in figure 3.

From the above observations, it was strongly suspected that these effects might be due to defects in the shape of the curved crystal i.e. due to improper elastic bending. Hence it was decided to carry out a Hartmann Test for the curved crystal, which has not been done earlier for this instrument.

Experimental procedure:

For the Hartmann test it was decided to scan the aperture of the

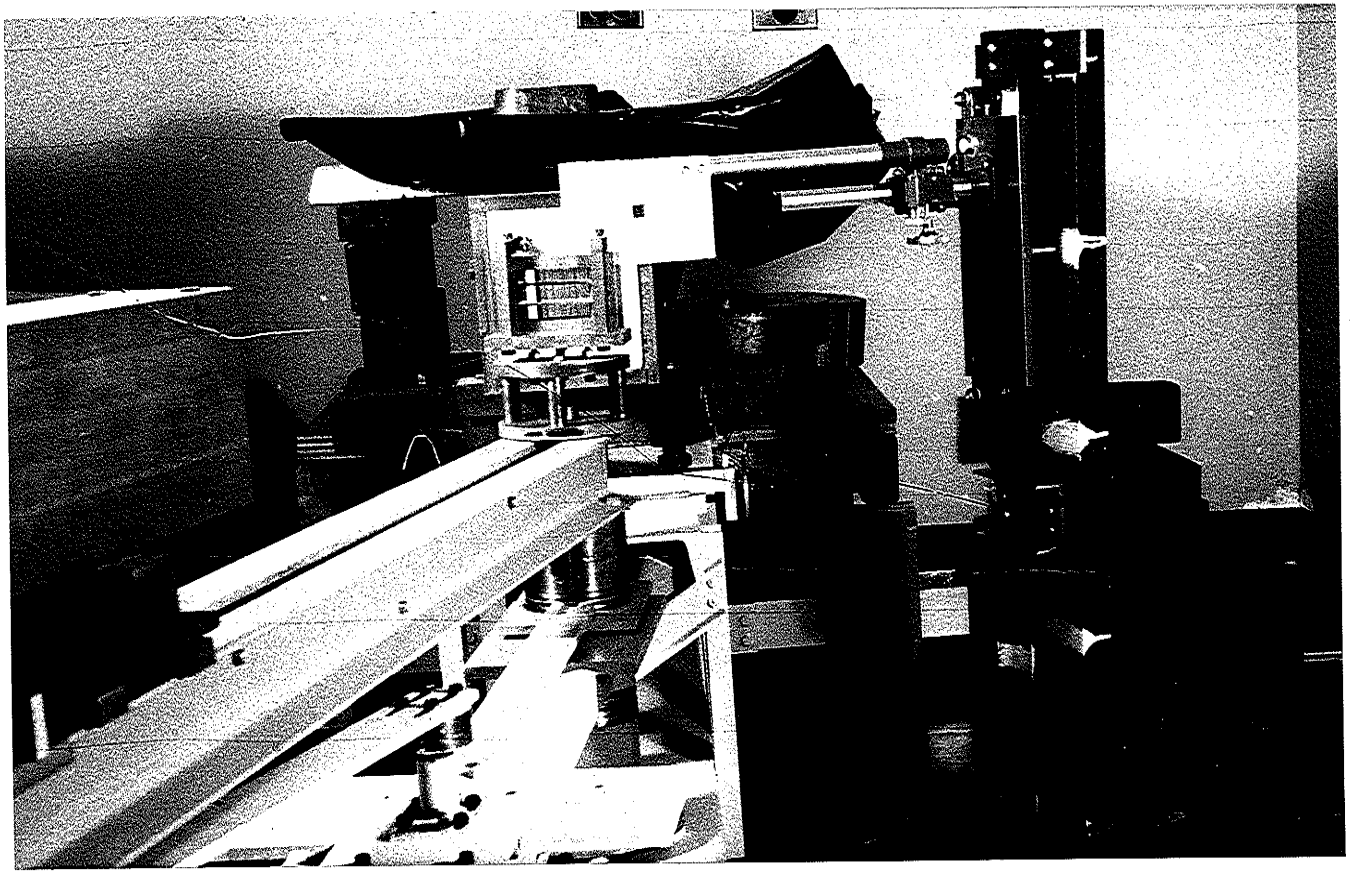

PLATE 2

Arrangement for scanning the crystal aperture (for Hartmann Test)

curved crystal with the help of some particular energy transition line and by subdividing the aperture into 15 equal parts; so that, by shielding the rest, only one-fifteenth of the whole aperture might be tested at a time.

For this purpose the 66.8 kev $K\alpha_1$(Pt) transition line of Iridium-192 was chosen with the following considerations. Of all transitions of Iridium-192, this gives the highest counting rate. As this transition is in the x-ray region, comparatively thinner (and so lighter) shielding material is needed. In fact, it was found that, less than a centimeter (about 0.8 cm.) in thickness of babbitt material was sufficient to reduce the intensity of this line to a negligible amount (about 1/1500 of the original intensity).

The dimensions of the crystal aperture are about 5.8 cm. by 4.8 cm. To scan it, a shielding plate of more than twice the aperture dimensions with an opening (about 1/15 of the total crystal aperture in area) at its centre was used. The shielding plate was made from babbitt about 1 cm. thick. It was made 14 cm. by 10 cm. with an opening 1.3 by 1.3 cm. at its centre.

The babbitt plate was fixed to one end of a cylindrical aluminum rod of about 25 cm. in length, the other end of which was clamped into the hollow cylindrical microscope holder of a laboratory microscope stand. This microscope stand was fixed to a vertical steel stand in such a way that the babbitt plate could be kept parallel to the vertical clamping block (which holds the curved crystal) and moved in a horizontal and vertical direction by moving the two microscope screws.

The babbitt plate was actually placed between the curved crystal and Soller slit system, parallel to and as close as possible (without interfering with the necessary movement of the clamping block holding

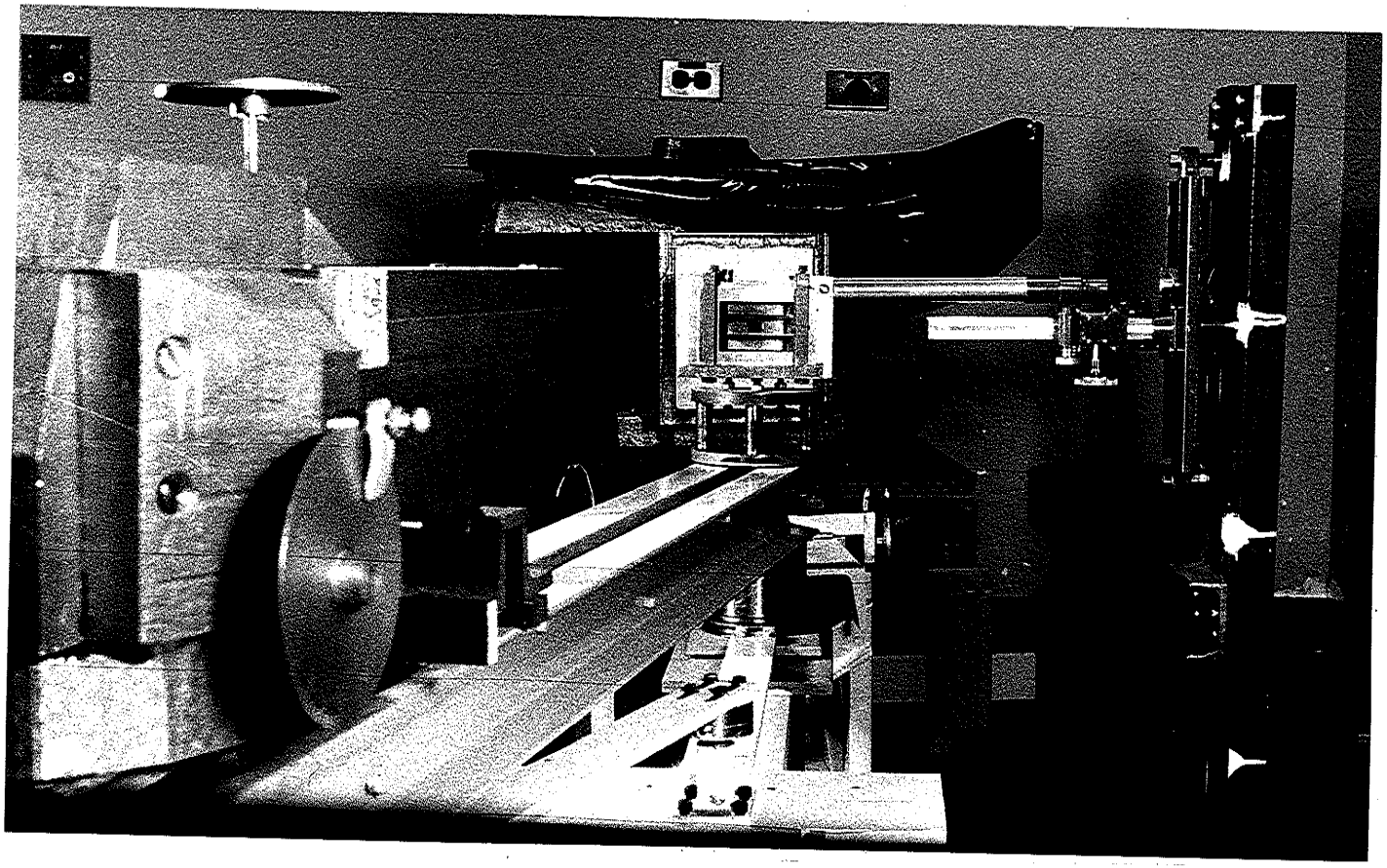

PLATE 3

Babbitt plate opening covering the M-3 region of the crystal aperture

(Source position is on the LEFT side)

THE UNIVERSITY OF MANITOBA LIBRARY

FIGURE 4

Top (T)	T-1	T-2	T-3	T-4	T-5
Middle (M)	M-1	M-2	M-3	M-4	M-5
Bottom (B)	B-1	B-2	B-3	B-4	B-5

15 subdivisions of the crystal aperture (for Hartmann Test).

(the curved crystal) to the convex side of the crystal. The whole arrangement is shown in plate 2.

Due to the two supporting parallel and horizontal steel ribs (2 cm. in depth and 1 mm. in height) of the clamping block, the crystal aperture was already divided into three strips of about 1.5 cm. in height and 5.8 cm. in length, which are named here as Top (T), Middle (M) and Botton (B) strips. By turning the microscope holder screw, which changes the position of the microscope in a vertical direction for an ordinary laboratory experiment, the central opening of the babbitt plate could be moved along each strip in a horizontal direction. So each strip was divided into five parts for this investigation which makes a total of 15 parts. The parts are named as illustrated in figure 4.

It may be noticed that, the babbitt opening is not exactly equal to 1/5 of the strips in area. Heightwise, a few millimeters of each sub-aperture is not covered for investigation; while, lengthwise each adjacent sub-aperture overlaps within a fraction of a millimeter. As the crystal is cylindrically bent lengthwise, a little overlapping of adjacent sub-apertures is useful so that no portion along the length of the crystal remains uninvestigated. The heightwise few millimeters uncovered portion is not very important, as it is unlikely that such portions will add any further information.

For each subdivision of the curved crystal aperture, spectral line profiles, resulting from reflection on both sides of the transverse planes, were drawn.

As the solid angle subtended at the source by each subdivision was smaller compared to the solid angle subtended by the full crystal aperture,

TABLE I

Data for 66.8 kev $K\alpha_1$ line with full crystal aperture

	Source Position LEFT	Source Position RIGHT
Maximum (peak) Intensity (counts per min.)	$62,900 \pm 200$	$62,200 \pm 200$
Full width at half maximum: in sec. of arc	36.2 ± 0.3	40.5 ± 0.6
Line position in dial reading	108.0	107.9

Source position left or right means left or right to an observer facing curved crystal from the 'zero' position of the spectrometer.

FIGURE 5.

Hartmann test data for the 15 subapertures of the curved crystal.

Variation in peak intensity

o-Intensity data obtained with source position on the LEFT side of an observer facing the crystal from the "zero" position of the spectrometer;
+-Intensity data obtained with source position on the RIGHT side of the same observer.

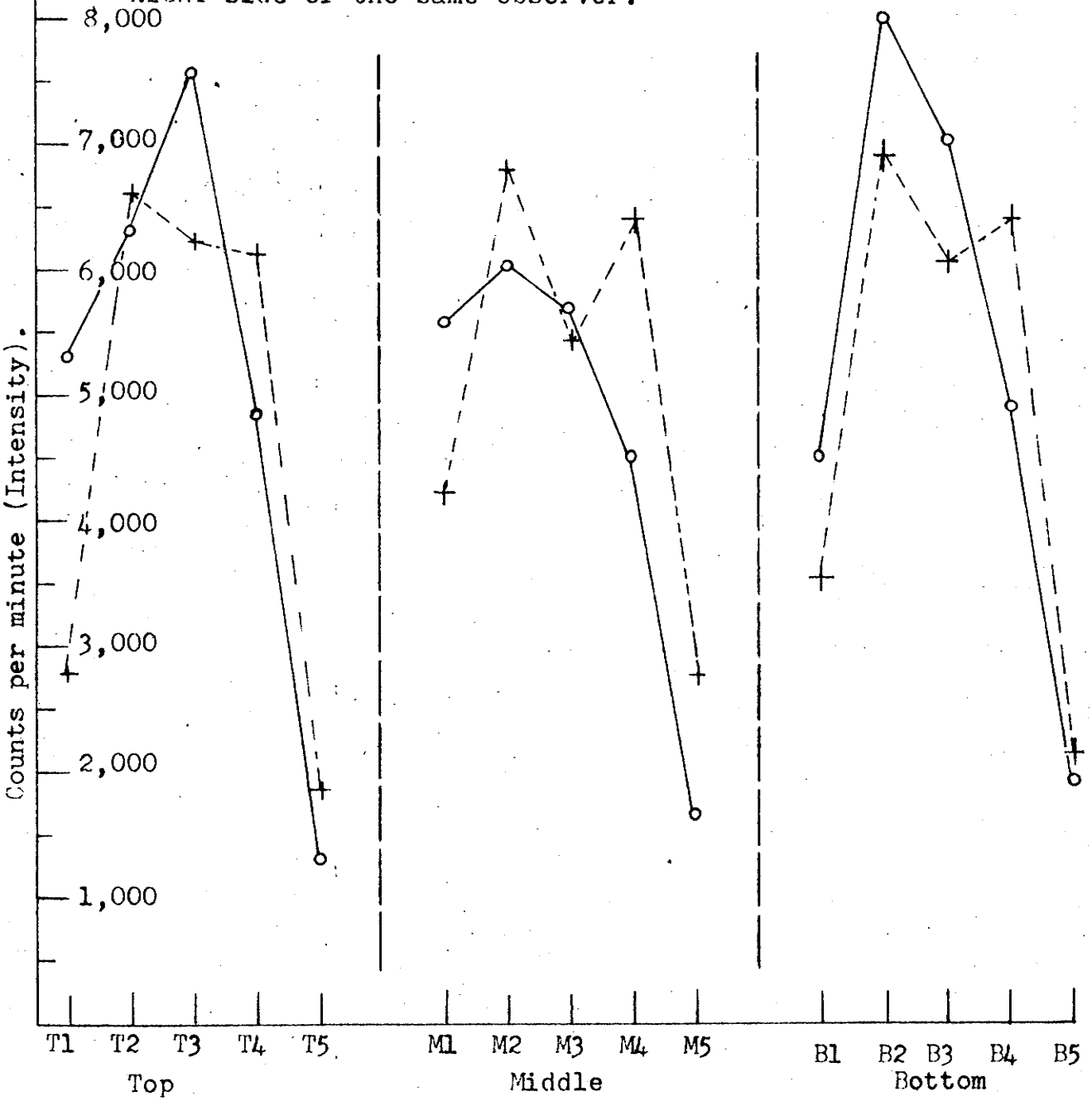

FIGURE 6.

Hartmann test data.

Full width at half maximum of the line profiles for 15 sub-apertures of the curved crystal, in seconds of arc.

o-Line width data for source position on LEFT.
+-Line width data for source position on RIGHT.

N.B. Values for T-5 and M-5 could not be determined due to ill shapes of their profiles.

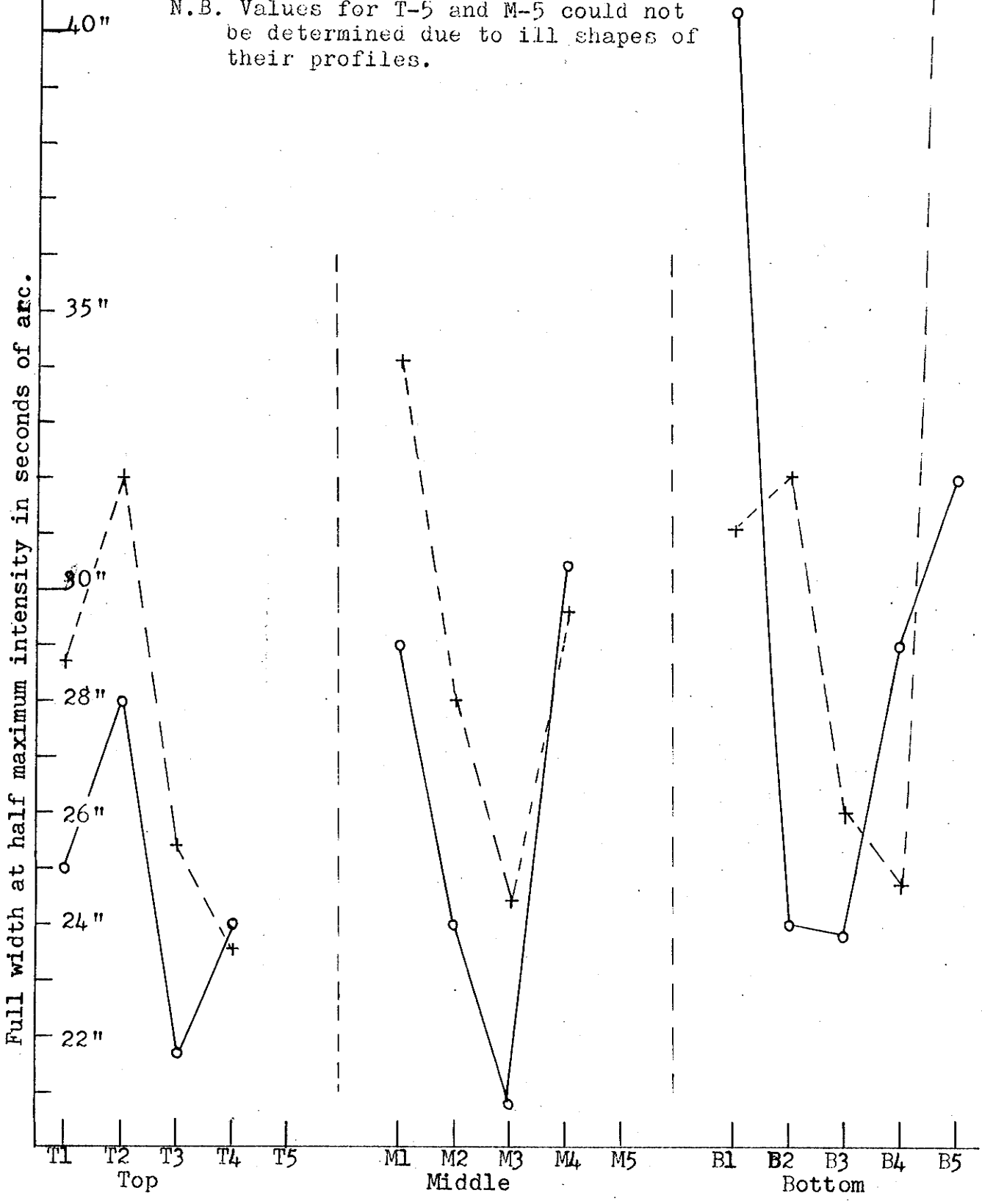

FIGURE 7.

Hartmann test data

Line positions of the profiles for 15 different sub-apertures of the curved crystal.

o-Data with source on LEFT.
+-Data with source on RIGHT.
Data for T-5 & M-5 could not be determined due to ill shapes of their profiles.

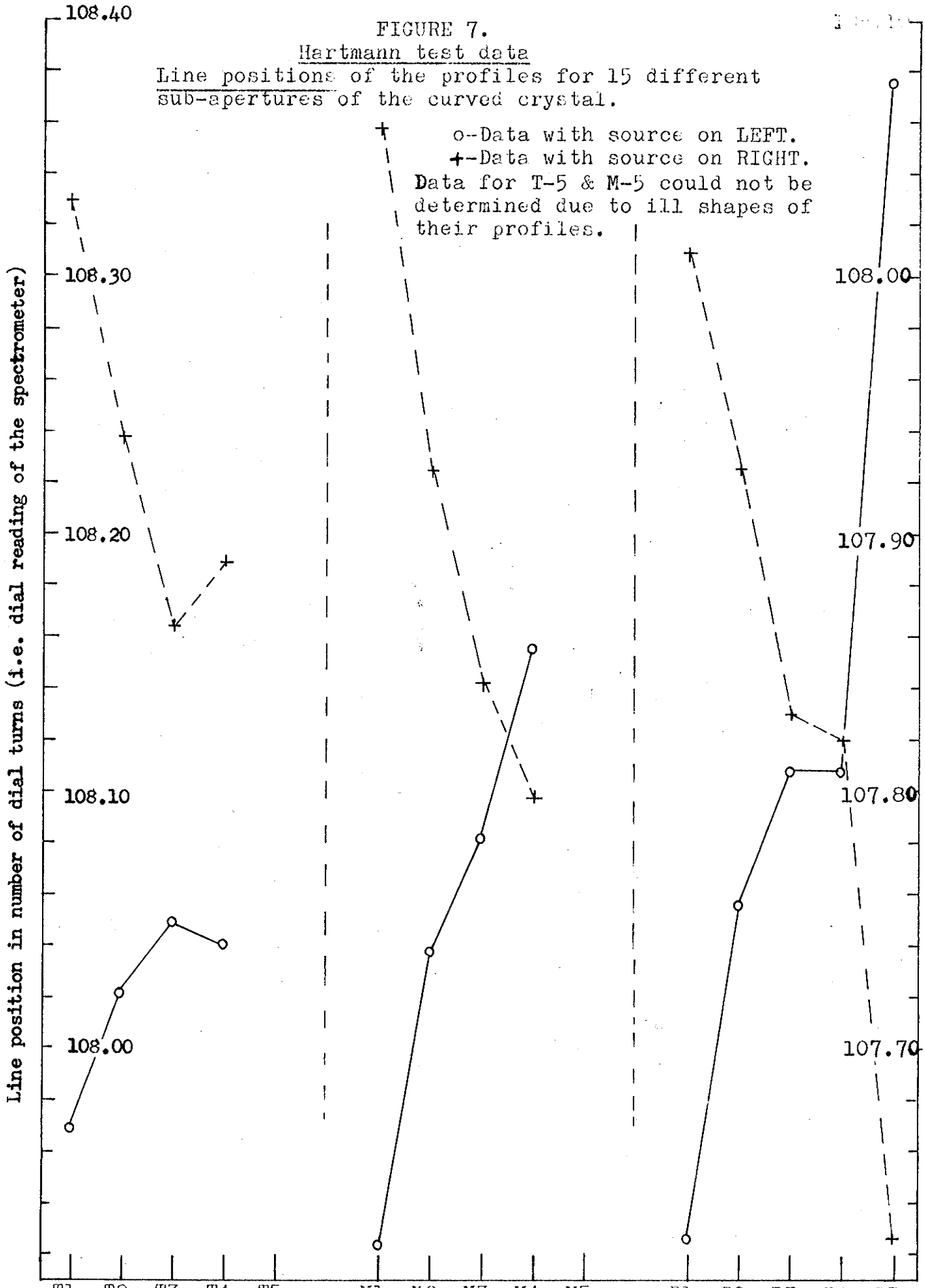

Right & Left side axes are for the Right & Left side data respectively.

the intensity was naturally expected to be much reduced. So, for the sake of good statistics, counts were taken for at least ten minutes for each position of the source.

Experimental observations.

Figures 5, 6, and 7, show the data obtained for each subdivision of the curved crystal aperture by studying the spectral line profiles resulting from reflection on the Left and Right sides (to an observer facing the crystal from the 'zero' position of the spectrometer) respectively of the transverse planes. Data obtained for the full crystal aperture are given in table I. Figures 5, 6, 7, and table I show the following data:

- Maximum (peak) intensity extrapolated (i.e. corrected for radioactive decay) to a particular day (3rd November, 1964).
- Full width of the line profiles at half maximum, $\delta\theta$, in seconds of arc.
- Line position of the profile in terms of the number of turns of the diffraction spectrometer dial from its zero position.

Values for $\delta\theta$ (figure 6) for right side studies are, in general, somewhat higher than the corresponding values for left side studies. For the line profiles with full crystal aperture, values for $\delta\theta$ in table I are 36.20 seconds and 40.45 seconds respectively. These data show that the line profiles obtained by reflection on the two sides of the transverse planes are not exactly mirror image of each other. This suggests that the instrument as a whole is, perhaps, not properly aligned.

Further, values of $\delta\theta$ for some parts of the crystal are much higher than that in some other parts, for the same side of the zero position. Some of the line profiles are so bad in shape, that $\delta\theta$ values for them

FIGURE 8.

HARTMANN TEST CURVES.
(Ref. page 16 Text.)

The 66.8 kev $K\alpha_1$ line profiles obtained by diffraction from the 15 different subdivisions of the curved crystal.

N.B. Curves show the shapes of line profiles only; correction has not been made for decay of the source, so intensities cannot be compared.

T-Top, M-Middle, B-Bottom.

R-Line profile for source position on the RIGHT side of an observer facing the crystal from the zero position of the spectrometer;
L-Line profile for source position on the LEFT side of an observer facing the crystal from the zero position of the spectrometer.

For explanation of T-1,....., M-1...., etc. see figure 4.

Hartmann Test curves.

FIG. 8.

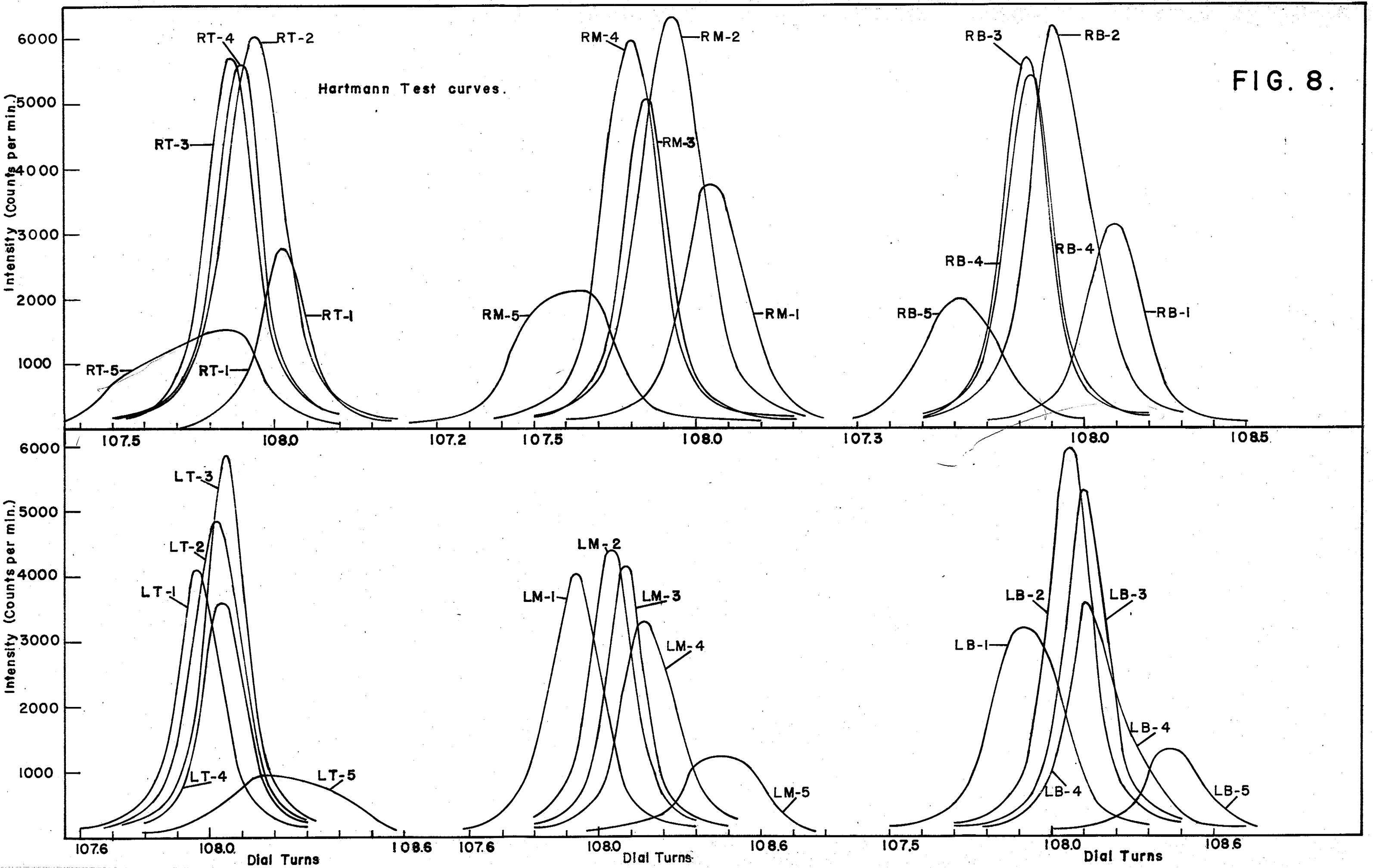

could not be ascertained. Such facts imply that the cylindrically bent crystal does not have a uniform curvature.

The following facts become apparent from a close study of the different line profiles (figure 8) obtained on reflection from both sides of the transverse planes for each subdivision of the full crystal aperture.

(For convenience, line profiles for different subdivisions and for left or right side are names as LT-1, LT-2,....; LM-1, LM-2,....; LB-1, LB-2,....; RT-1, RT-2,....; RM-1,....; etc.)

(1) Line positions of the profiles for the top part of the crystal (i.e. LT and RT profiles) are closer. This is not so for the line profiles for the middle or the bottom parts of the crystal.

(2) Shapes of the line profiles can, in general, be classified under four heads: (a) Symmetrical and sharp (narrow), (b) Symmetrical and wide (broad), (c) Unsymmetrical and wide (broad), (d) Ill shaped.

(a) Symmetrical and sharp:

LT-1, LT-3, LT-4, LM-2, LM-3, LB-2 and LB-3 line profiles are fairly symmetrical. Their $\delta\theta$ values vary from less than 21 seconds to 25 seconds of arc.

RT-3, RT-4, RM-3, RB-3 and RB-4 line profiles are symmetrical, (though less symmetrical compared to their counter parts on the left side), and broader. Their $\delta\theta$ values vary from about 23.5 seconds to 26 seconds of arc.

(b) Symmetrical and wide:

LT-2, RT-1, RT-2, RM-4 and RB-1 line profiles are fairly symmetrical and wide. Their $\delta\theta$ values vary from 28 seconds to 32 seconds of arc.

(c) Unsymmetrical and wide:

LM-1, LM-4, LB-1, RM-1, RM-2 and RB-2 line profiles are more or less unsymmetrical and wide. Their $\delta\theta$ values vary from 28 seconds to 40.5

seconds of arc.

(d) Ill shaped:

LT-5, LM-5, LB-4, LB-5, RT-5, RM-5 and RB-5 profiles are ill shaped. LB-4 shows a slanting straight line tail on its lower energy side. T-5, M-5 and B-5 profiles (L and R) are very poor in shape, have unusually broad peaks and much reduced intensities.

From such facts it appears that, --

(i) Top strip of the crystal (T-1 to T-4) is comparatively more uniform in curvature than the rest of it. (So line profiles for these parts are comparatively better in shape and closer.)

(ii) T-3, M-3 and B-3 regions (that is, the central part of the cylindrically bent crystal) are uniform in curvature.

(iii) M-1 is not a good part of the crystal.

(iv) T-5, M-5, and B-5, which are on one side of the crystal, are the worst parts.

(v) Utility of M-2, M-4, B-1, B-2, and B-4 parts is doubtful. Information from left and right side studies for these parts are contradictory.

(vi) Shapes of the left side line profiles are, in general, better, compared to their counter parts on the right side.

(Hartmann test experiments for all the 15 parts have been repeated. This was done to verify the accuracy of the data, but no noteworthy discrepancy could be observed.)

For the left side study, as well as for the right side study, (when the centre of curvature of the bent crystal was on the left and right sides of the zero position respectively), the babbitt plate was placed as parallel to and as close as possible to the convex side of the crystal. Care was taken to see that the babbitt plate did not interfere with the rotational movement (due to change in source position) of the clamping block holding the

FIGURE 9.

Hartmann Test Curves

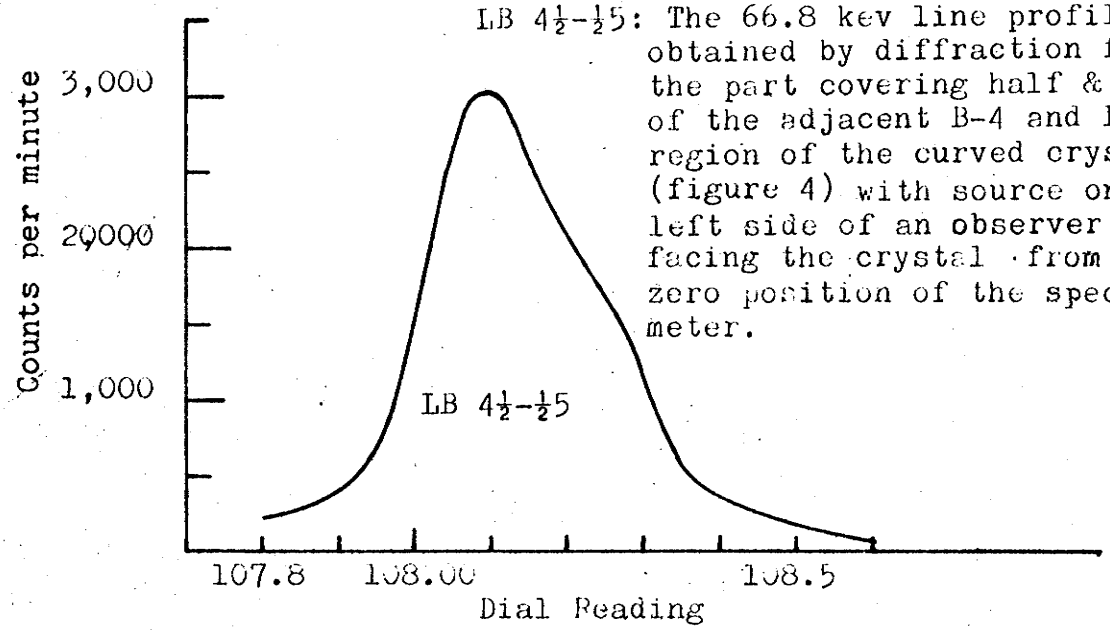

LB $4\frac{1}{2}-\frac{1}{2}5$: The 66.8 kev line profile obtained by diffraction from the part covering half & half of the adjacent B-4 and B-5 region of the curved crystal (figure 4) with source on the left side of an observer facing the crystal from the zero position of the spectrometer.

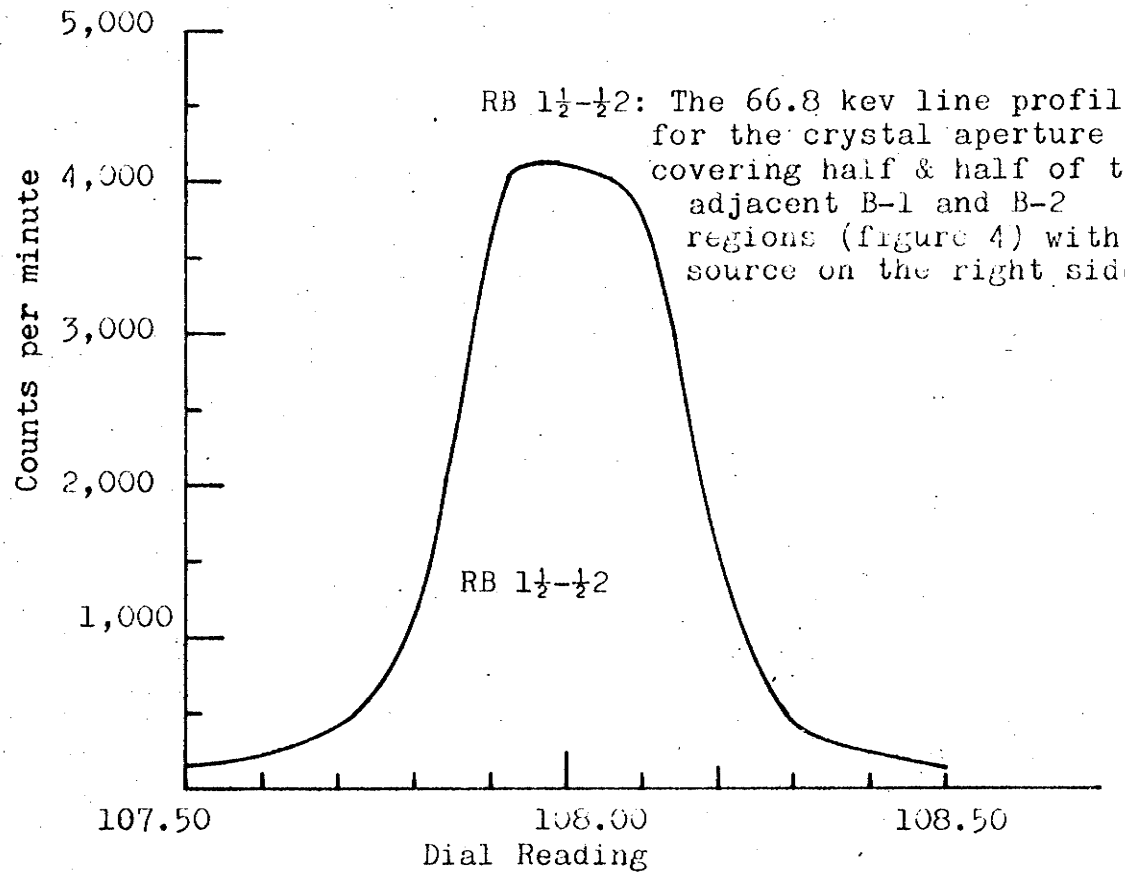

RB $1\frac{1}{2}-\frac{1}{2}2$: The 66.8 kev line profile for the crystal aperture part covering half & half of the adjacent B-1 and B-2 regions (figure 4) with source on the right side.

The counterparts of these two curves, with source positions on the other sides, show similar poor shapes.

crystal. As a result, for changing over from left to right side study, it was necessary to remove the babbitt plate from its position and then replace it; otherwise, it would interfere with the free movement of the clamping block. The whole arrangement was a crude one. The removal and replacement of the babbitt plate was manually operated. Only unaided eye could be used to judge how close and how parallel the babbitt plate and the clamping block are. Thus there is every likelihood that, the respective subdivisions examined on the left and right sides did not cover exactly the same parts of the crystal aperture. However, this has not turned out to be any disadvantage. The gross disagreement between the left and right side line profiles for the parts mentioned above, indicate that the crystal is distorted somewhere at the borders of M-1, and M-2, M-4 and M-5, B-1 and B-2, and B-4 and B-5. Therefore, as a next step, line profiles were drawn for parts covering borders of these adjacent subdivisions for both sides (Right and Left). For the middle parts such profiles merely revealed that the distortions of M-1 and M-5 regions extend by a few millimeters into the respective adjacent regions M-2 and M-4; but for the bottom parts these line profiles showed some interesting features. Line profiles for parts covering half of B-1 and half of B-2, and half of B-4 and half of B-5 taken on the right and left respectively are shown in figure 9. They have been named as RB1$\frac{1}{2}$-$\frac{1}{2}$2 and LB4$\frac{1}{2}$-$\frac{1}{2}$5 respectively. Both of them have poor shapes. While LB4$\frac{1}{2}$-$\frac{1}{2}$5 show a distorted shape, RB1$\frac{1}{2}$-$\frac{1}{2}$2, show a broad and flat peak.

Later, line profiles for B$\frac{1}{2}$1 and B5$\frac{1}{2}$ (i.e. the regions nearer to the vertical sides of the clamping block and approximately half in area of B-1 and B-5 regions) were drawn. These profiles are symmetrical in shape, though fairly broad and low in peak intensities.

FIGURE 10

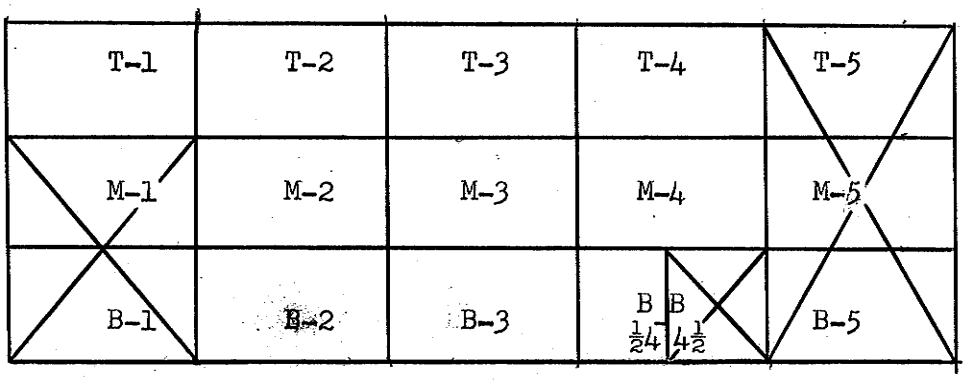

15 subdivisions of the crystal aperture.

Crosses show the parts deleted (with the help of lead blocks) for obtaining better shaped line profiles.

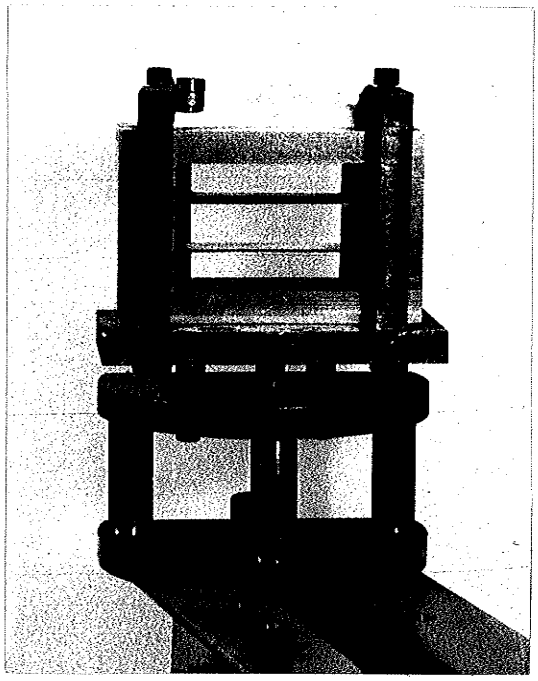

PLATE 4A

Original Crystal Aperture

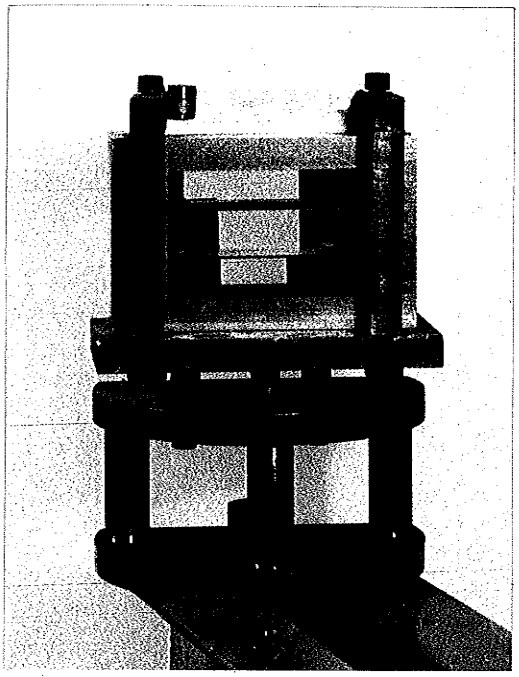

PLATE 4B

Improved Crystal Aperture

TABLE II

Comparison of Data from Gamma Energy Line Profiles Taken

Before and After the Improvement of the Crystal Aperture

Spectral Energy line in kev unit E	Data taken with Original Crystal Aperture: Spectral line position in dial turns	Maximum counts per min. (Background deleted) C_o	Full width at half maximum in seconds of arc W_o	Data taken with Improved Crystal Aperture: Spectral line position in dial turns	Maximum counts per min. (Background deleted) Ci	Full width at half maximum in seconds of arc Wi	Ratio of maximum counting rates Ci/Co	Ratio of full widths at half maximum Wi/Wo
66.8			36.2 ± 0.3			29.9 ± 0.3		
201	35.8	1,680 ± 50	25.0 ± 1.2	35.8	1,500 ± 30	19.6 ± 1.2	0.89	0.78
206	35.0	10,640 ± 100	22.3 ± 0.6	35.0	9,900 ± 80	15.4 ± 0.6	0.93	0.69
283	25.4	330 ± 25	21.7 ± 3.0	25.5	320 ± 20	18.1 ± 2.4	0.95	0.83
296	24.3	30,450 ± 150	22.0 ± 0.3	24.4	25,800 ± 100	19.3 ± 0.3	0.85	0.88
308.5	23.3	27,700 ± 200	23.2 ± 0.3	23.4	24,450 ± 100	20.8 ± 0.6	0.88	0.90
316.5	22.7	70,000 ± 300	23.5 ± 0.3	22.8	62,400 ± 170	20.2 ± 0.3	0.89	0.86
375	19.2	360 ± 10	21.4 ± 1.8	19.3	300 ± 20	18.4 ± 1.2	0.85	0.86
416.6	17.2	250 ± 6	26.2 ± 3.6	17.3	210 ± 10	20.2 ± 1.8	0.86	0.77
468	15.3	10,490 ± 100	22.9 ± 0.6	15.4	9,630 ± 50	19.0 ± 0.5	0.92	0.83
484.6	14.8	670 ± 15	26.8 ± 2.4	14.9	600 ± 20	19.9 ± 1.2	0.90	0.74
Average			23.5 ± 1.4			19.1 ± 1.0	0.89	0.81

Average reduction in: Maximum counting rate 11%
Full width at half maximum 19%

N.B. Maximum counts have been extrapolated to a zero day (October 10th, 1964) i.e. have been corrected for the decay of the source. As a comparison of x-ray and gamma-ray line widths, the widths of 66.8 kev line have been shown in this table, but they have not been considered for averaging purposes.

From these observations it can be concluded that,

(1) As the left side line profiles are better in shape than the right side ones, for relative intensity measurement it is advisable to take spectra on the left side only.

(2) In order to obtain fairly sharp and symmetrical line profiles, it is necessary to delete certain parts of the crystal.

Improvement of the aperture:

The next problem was to find a better aperture of the curved crystal (by deleting certain parts) for which more symmetrical and sharper (i.e. narrower) line profiles would be obtained. For this purpose, combinations of different parts of the crystal were deleted (with lead blocks) and line profiles obtained with such apertures were studied. Consideration was given to the fact that loss in intensity (due to reduction in aperture area) should be compatible with gain in resolution.

After trials it was found that deletion of T-5, M-5, B-5 half of B-4 adjacent to B-5, M-1, and B-1 parts gave reasonably better shaped (sharper and more nearly symmetrical) line profiles, without much loss in the counting rate.

These parts were blocked with lead pieces about $1\frac{1}{2}$ inches thick, which were sufficient to reduce (by about 1/1000) the intensities of gamma rays up to 613 keg. About 37% of the whole crystal aperture was deleted. Figure 10 shows the improved crystal aperture.

Results of improvement of the curved crystal aperture can be easily understood from Tables II and III.

From Table II it can be observed that due to reduction in aperture area counting rates and widths of the line profiles have been reduced. For the energy range of 201 kev to 484 kev, average reduction in counting rate is 11%,

FIGURE 11.
613kev, 605kev & 589kev line profiles.
B-Before improvement and A-After Improvement
of the curved crystal aperture.

Extended (dashed) lines, showing boundary of each of the three line profiles, have been drawn on the basis of the symmetry observed in line profiles obtained with improved aperture.

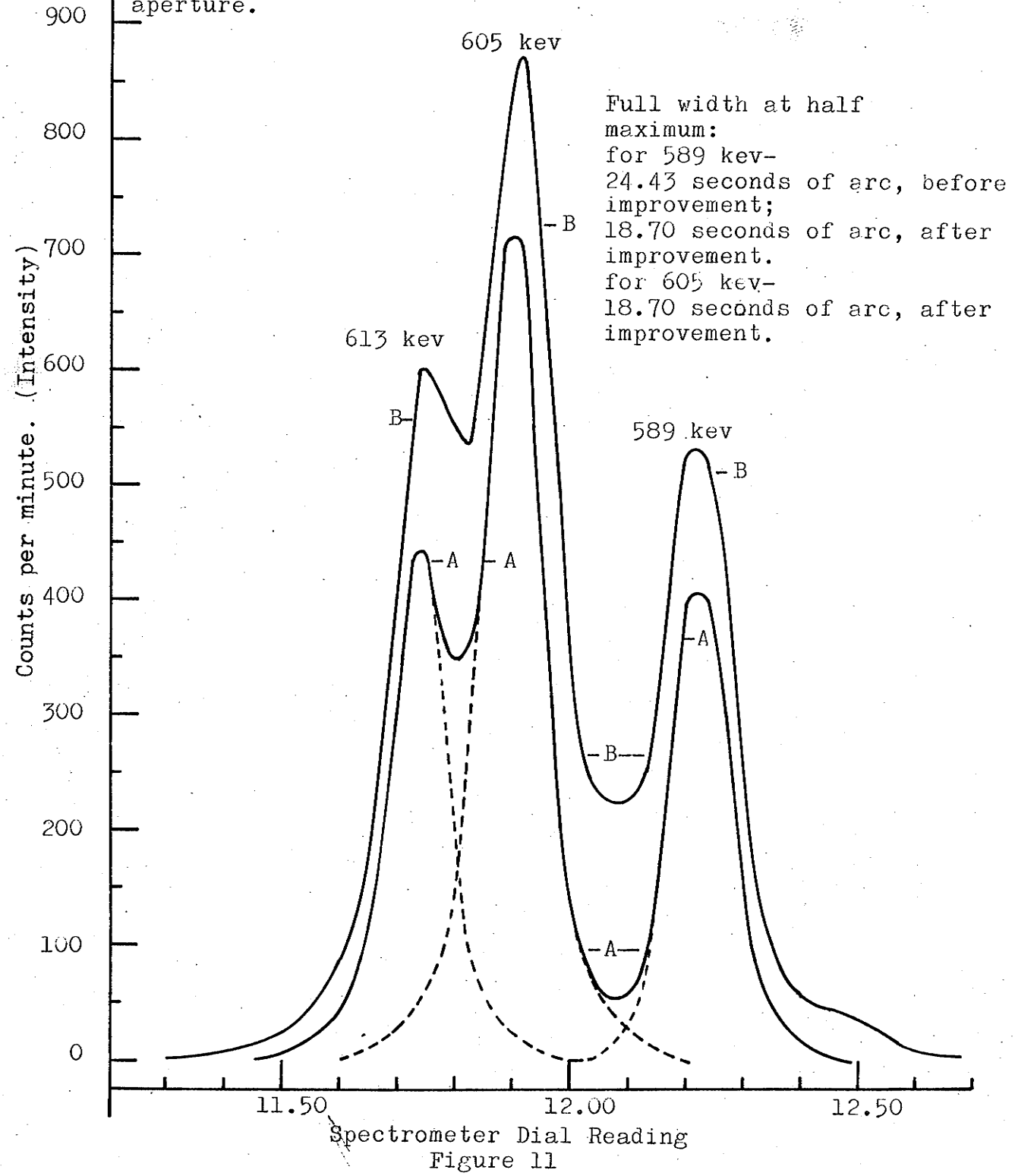

Figure 11

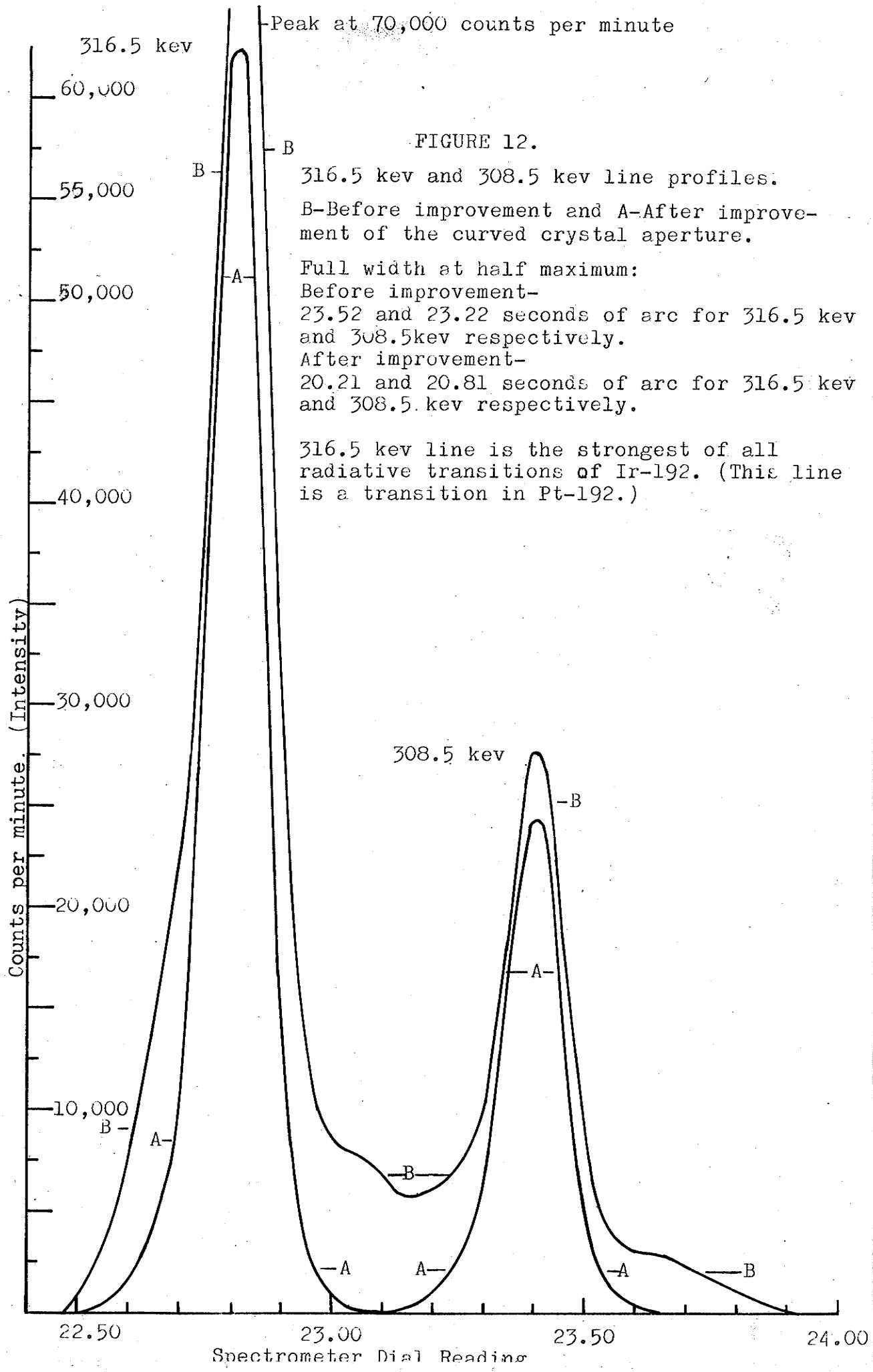

FIGURE 12.

316.5 kev and 308.5 kev line profiles.

B-Before improvement and A-After improvement of the curved crystal aperture.

Full width at half maximum:
Before improvement-
23.52 and 23.22 seconds of arc for 316.5 kev and 308.5kev respectively.
After improvement-
20.21 and 20.81 seconds of arc for 316.5 kev and 308.5 kev respectively.

316.5 kev line is the strongest of all radiative transitions of Ir-192. (This line is a transition in Pt-192.)

TABLE III

Showing the Effect of Improvement
in Resolution of Adjacent Line Profiles
as a Result of Improved Crystal Aperture

Spectral energy line in kev unit E	Data Taken with Original Aperture: Peak height (counts per minute)	Adjacent valley height (counts per minute)	Ratio 1 peak height / valley height	Data Taken with Improved Aperture: Peak height (counts per minute)	Adjacent valley height (counts per minute)	Ratio 2 peak height / valley height
201	1,680	84	20.00	1,496	0 (nil)	
206	10,640	84	126.70	9,920	0 (nil)	
308.5	27,700	5,800	4.78	24,450	300	81.50
316.5	70,000	5,800	12.07	62,400	300	208.0
468	10,490	75	139.90	9,630	29	332.10
484.6	335	75	4.47	298	29	10.30
589	530	218	2.43	400	48	8.25
605	872	218	4.00	714	48	14.90
605	872	536	1.65	714	344	2.08
613	600	536	1.12	442	344	1.29

Peak height is the highest point of a line profile.
Valley height is the lowest point between two adjacent peaks.(For examples, see figures 11 and 12.)

Peak height and valley height counting rated have been obtained from the actual line profiles. So, statistical error has not been quoted here. These heights (counting rates) are background deleted data.

and the average reduction in full width at half maximum is 19%.

Full widths at half maxima show wide variation (Table II). Particularly the value 15.4 ± 0.6 sec. of arc for 206 kev line, taken with improved aperture, is much lower than the average value 19.1 ± 1.0 sec. of arc. Mechanical defects in the instrument may be a cause for such random variation. Due to limitation of time this could not be investigated further.

Table III shows peak to valley ratio for two adjacent line profiles. These data have been obtained from the drawn out line profiles and are background deleted data. Determination of background have been explained in Chapter IV, under the section, "Procedure (Experimental)." It is apparent from this table that, due to improved aperture two close gamma lines are much better resolved than before. Figures 11 and 12 show direct comparison of some of the adjacent line profiles drawn with original and improved aperture of the crystal. Valley is the lowest point of the curve between the adjacent peaks (e.g. 613 and 605 kev, 605 and 589 kev and 316.5 and 308.5 kev).

Discussion:

Ill shaped profiles.

An attempt to present plausible reasons for irregular shapes of Hartmann test line profiles is made here.

To begin with, let the case for an ideal line profile be considered. (An ideal line profile is the profile of an x-ray

FIGURES 13, 14 and 15.

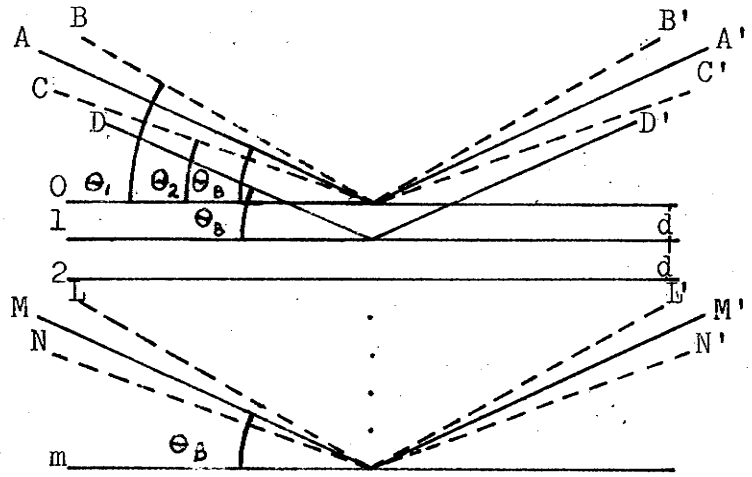

Figure 13.
(Ref. page 20 text)

Figure 14.

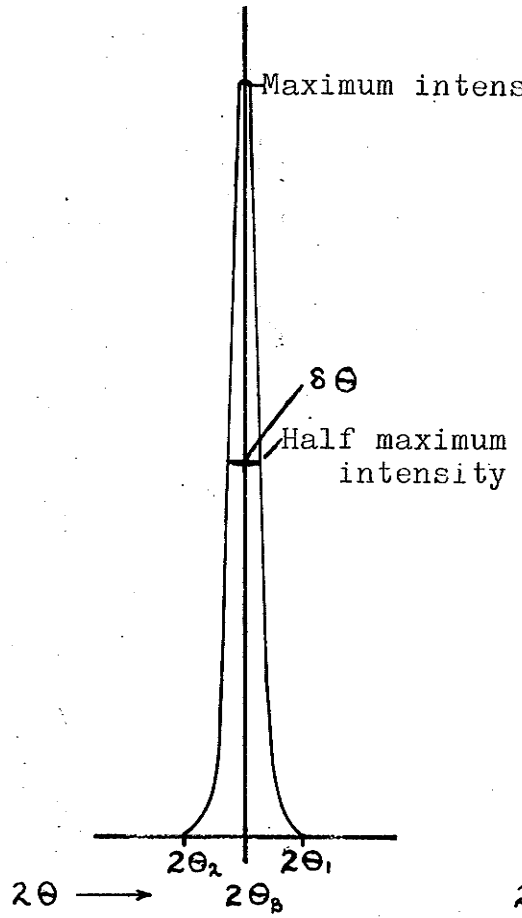

Fig. 14(Ref. page 21 text).

Figure 15.

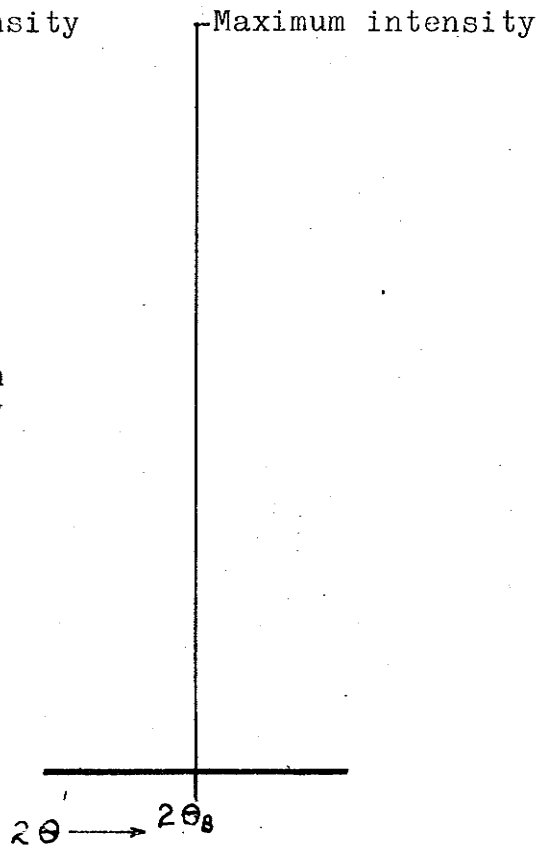

(Ref. page 21 text)Fig.15.

or gamma ray obtained by diffraction through an infinitely thick, perfect (i.e. without any lattice defect) and unstrained crystal.)

Let there be a set of (m + 1) Bragg planes in a perfect and plane diffracting crystal with a Bragg spacing d. Let the angle at which Bragg's law ($n\lambda = 2d \sin\theta$) for x-ray (or gamma ray) reflection is exactly satisfied be called θ_B. Then incident rays making this angle with the Bragg planes will meet in the same phase after reflection and so, will satisfy the condition of <u>constructive</u> interference. In figure 13, rays A, D, ..., M are such rays.

Rays, which are ($n + \frac{1}{2}$) wavelengths (where n is any integer including zero) out of phase, will satisfy the condition of destructive interference.

When rays emitted from a source are studied, not all rays will satisfy the ideal cases mentioned above. For rays making angles slightly different from θ_B with the Bragg planes, the case may be as follows.

In figure 13, rays B, ..., L make the angle θ_1, and rays C, ..., N, make the angle θ_2 with the Bragg planes (0, ..., m). θ_1 is slightly greater than and θ_2 is slightly smaller than θ_B. Let the angles θ_1 and

θ_2 be such that the rays L' and N' from the m^{th} plane be (m + 1) and (m - 1) wavelengths out of phase with B' and C', the rays from the surface plane, respectively. Then, midway in the crystal there can be some plane reflecting a ray which is $(n + \frac{1}{2})$ wavelengths out of phase with the ray B' from the surface plane. These rays cancel each other. Similarly, another ray from that midway plane can interfere destructively with the ray C' from the surface plane. This means that, rays from such pair of planes throughout the crystal can cancel one another. The net effect is, - rays from planes in the top half of the crystal annul those from planes in the bottom half of the crystal. So intensity of the beams diffracted at an angle $2\theta_1$, or $2\theta_2$ is therefore, zero. Under the condition, diffracted intensity at an angle near $2\theta_B$, but not greater than $2\theta_1$, or less than $2\theta_2$, is not zero. The diffracted intensity can have some value in between zero and the maximum intensity at the diffraction angle $2\theta_B$. The curve of diffracted intensity versus 2θwill thus have the form given in figure 14 in contrast to figue 15, which illustrates the hypothetical case of diffraction occuring only at the exact Bragg angle.

As a rough measure of the full width at half maximum $\delta\theta$, we can take half the difference between the two extreme angles at which the intensity approaches zero, or $\delta\theta = \frac{1}{2}(2\theta_1 - 2\theta_2) = \theta_1 - \theta_2$.

For an ideally bent crystal, rays emanating from one and the same point on the focal circle will encounter the crystal slab so as to satisfy the Bragg condition at all points throughout its entire thickness for one and the same wavelength. In order that reflections from a number of different atomic planes may co-operate coherently, it is necessary that rays starting from a source point (an emitting atom), after reflection on different planes, shall, by different paths, eventually reunite at an

observation point (an absorbing atom in the detecting system). The interference (i.e. superposition of wavelets) does not in reality occur in the crystal but at the point of observation.

If, due to defects (e.g. uneven curvature) in the clamping block, the crystal is improperly bent, so that radii of curvatures of various parts (within any subdivision) of the crystal differ widely, then the ideal condition referred to above, will not be satisfied. In such a case, the anomalous reflected rays will have less chance to interfere with each other. This will cause distortion in the shape of the line profiles.

Particularly, if some parts have much less curvature, that is, if some parts are comparatively more flat, then the picture will be as follows.

Transverse crystal planes (which are perpendicular to the crystal surface) for such parts will be, to some extent, parallel, in-stead of converging to any point. Consequently, rays, emitted from the source on the focal circle and reflected by these crystal planes, will have much less chance for transmission through the baffle collimator, as such rays will in general be reflected in heterogeneous directions. Moreover, in such a case there will hardly be any particular position of the source for which only, the Bragg relation can be satisfied. Instead, as the spectrometer dial is turned, for each position of the source (within, of course, a limited range) there will be nearly the same probability of the Bragg relation being satisfied for some part of the crystal. So, instead of a peak, the diffracted line profile will show a broad or flat top and an extended rise or decay. Compared to well shaped line profiles such profiles will be broad and reduced in intensity, because there will not be any particular position of the source for constructive interference

of the rays. Reduction in intensity will also be due to a smaller number of rays being transmitted through the baffle collimator. Best examples of such profiles are B1½-½2, T-5 and M-5. (Figures 8 and 9.)

In order to achieve an even curvature, an equal but opposite torque must be applied to the opposite sides of the crystal lamina by the clamping blocks. The experimental observations show that T-5 and M-5 parts are comparatively more flat but T-1 and M-1 parts are not so. This suggests the following possibilities:

(1) The curvature of the clamping blocks may not be uniform.

(2) The crystal lamina may not be exactly a rectangular piece and/or the crystal lamina might not have been mounted symmetrically inside the clamping blocks. (If one end of the lamina is just anchored in the blocks, then little torque is applied to that end. The result is, much less curvature compared to the other end. It may be that the crystal lamina is little more than anchored at T-5, M-5, B1½-½2 (adjacent halves of B-1 and B-2) and, to some extent, B4½-½5 (adjacent halves of B-4 and B-5) edges; whereas, edges of the other parts of the crystal lamina are well within the clamping blocks.)

Right side profiles.

It has been observed that right side profiles are broader in general and less symmetrical than the corresponding left side ones. The reason for this is not very clear. However, it may be possible that, the instrument as a whole is not properly aligned. Perhaps, on the left side the slit source moves closer to the actual focal circle, than on the right side. In such a case, the geometry of the instrument for proper focussing will be less accurate on the right side, and so, for any particular position of the source, rays emitted by it will not be incident on the different transverse crystal planes at the same grazing angle. As

a result, spectral profiles will be diffused or broad and unsymmetrical.

Line positions.

Line position of a gamma ray or x-ray profile is taken as a measure of the exact Bragg angle of diffraction for that ray.

For a perfectly bent crystal (which should have only one centre of curvature for all different parts of its surface) Bragg angle for any particular wavelength should not change for diffraction through different parts of the crystal.

For ill shaped profiles, line positions could not be determined with any accuracy. For better shaped profiles it has been observed that, line positions are not very close. (Figure 7.)

Variation in line positions suggests that the whole crystal lamina is not oriented in the shape of one right circular cylinder. Curvature changes from part to part.

Line widths.

Spectral profile obtained by diffraction from a perfect crystal will have certain line width (full width at half maximum). Reason for this has been explained at the beginning of this 'Discussion' section.

Other factors contributing towards line width are,-

(1) Finite breadth of the source.

(2) Crystal imperfection known as mosaic structure, which is possessed to a lesser or greater extent by all real crystals. This has a decided effect on diffraction phenomena. (A crystal with mosaic structure does not have its atoms arranged on a perfectly regular lattice extending from one side of the crystal to the other; instead, the lattice is broken up into a number of tiny blocks, each slightly disoriented one from another.)

(3) Curvature of the crystal.

J. W. Knowles, in his article 'Crystal Diffraction Spectroscopy of

Nuclear Gamma Rays', mentions that, - "Prior to bending, an unstrained quartz crystal lamina has been shown, by double crystal diffraction, to have a distribution of crystalline mosaic of only 1 to 3 seconds of arc. When elastically bent, the diffraction line width increases from a few seconds to 13-20 seconds of arc depending on the radius of curvature of the crystal." (Alpha, Beta and Gamma Ray Spectroscopy, Volume 1, page 221.) So the observed variations in line width, $\delta\theta$ (figure 6) are possibly indication of variations in curvature from part to part of the crystal.

Intensities.

From Figure 5, it can be observed that, maximum intensities for different subdivisions vary. In addition to statistical variations, there may be two possible reasons for this.

(1) Due to imperfection of curvature, rays diffracted from different subdivisions of the crystal cannot necessarily have the same transmission probability through the baffle collimator, because, variations in curvature from part to part can cause variations in the direction of diffracted rays.

(2) If the baffle system is not perfect, that is, if the fifty baffle slots are not heightwise parallel to each other and do not (lengthwise) converge to a point (if extended), then each of these slots cannot have the same transmission probability. The babbitt plate opening, which subdivides the crystal aperture, necessarily subdivides the baffle collimator aperture also. Any irregularity of the slots falling within such subapertures of the baffle collimator will greatly affect transmission of the diffracted gamma rays.

Variation of maximum intensities for the same subdivision, for left and right hand study, is not difficult to follow. It has been already

Figure 16. Transmission of diffracted X-rays (66.8 kev) through the baffle collimator (Soller slit system).

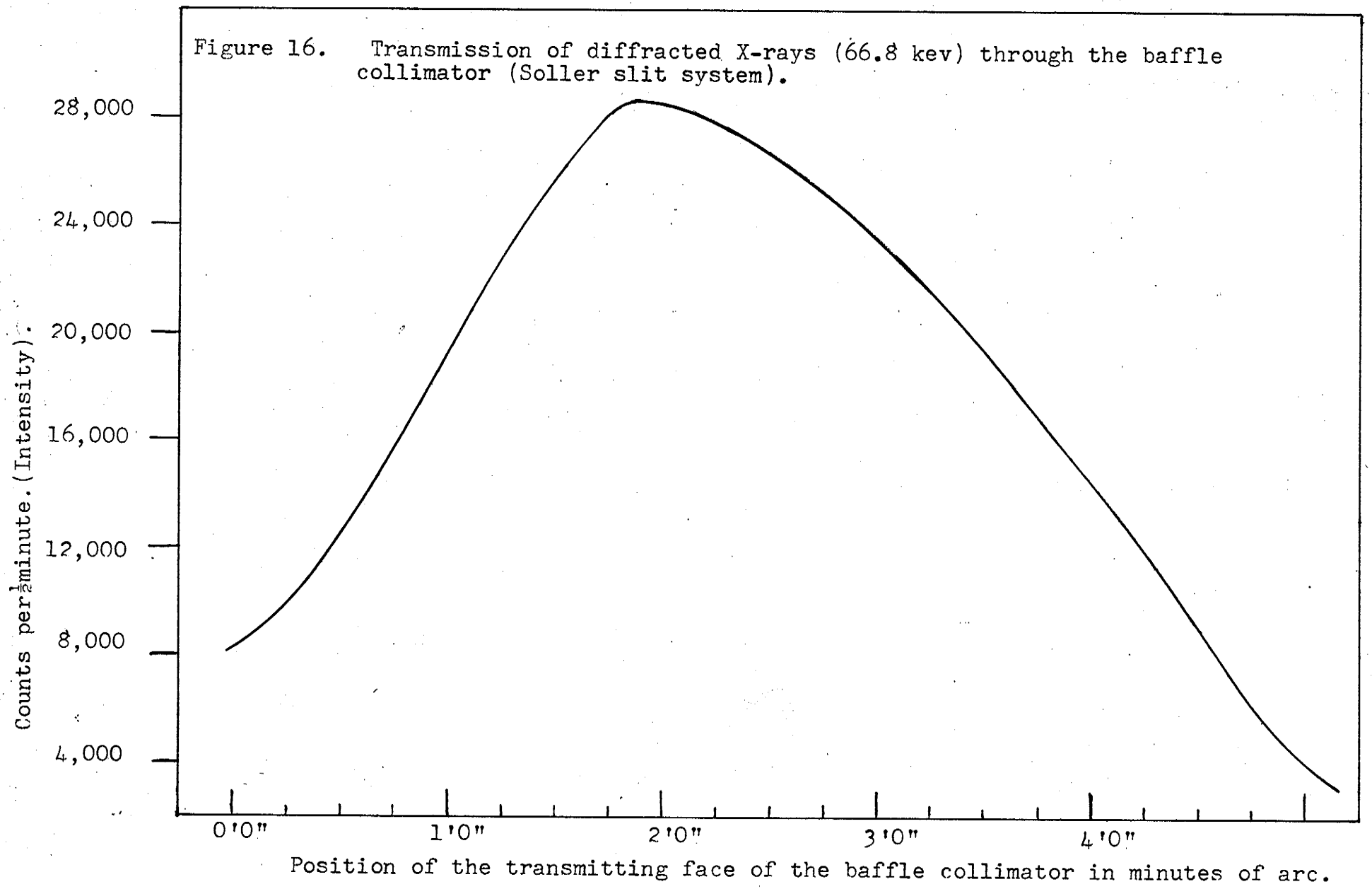

The starting point (0'0") is arbitrary and on the RIGHT side of an observer facing the baffle collimator from the source position.

FIGURE 17

Top	OT-1	OT-2	OT-3	OT-4	OT-5	OT-6	OT-7
Middle	OM-1	OM-2	OM-3	OM-4	OM-5	OT-6	OT-7
Bottom	OB-1	OB-2	OB-3	OB-4	OB-5	OB-6	OB-7

21 subdivisions of the crystal aperture for the optical test of the crystal curvature.

pointed out that, for left and right side studies the same subdivisions do not cover exactly the same areas of the curved crystal and of the baffle collimator aperture. (It has actually been observed that, a lateral displacement of the babbitt opening by a millimeter can make a change in the counting rate by about 10 to 15 per cent. Such observations have been made with babbitt opening covering good parts of the crystal.)

A detailed study of the transmittivity of the baffle collimator, though intended, could not be carried out, as it was not desirable to remove the curved crystal from its present position.

At the beginning of the Hartmann test experiments, an attempt was made to find out the best transmittivity position of the baffle collimator with full crystal aperture. This was done by turning the screw which moves the collimator aperture (nearer to the curved crystal) laterally. For getting readings, a graduated circular disc was fitted to this screw head. The source was placed at the maximum intensity position of the 66.8 kev line. The intensity versus collimator position (in terms of minutes of arc) curve is shown in figure 16. This curve shows that transmittivity of the baffle system decreases more gradually on the left side (facing collimator aperture from the source position) of the maximum transmittivity position than on the right side.

The baffle collimator was placed at the maximum intensity position according to this curve for all experimental investigations reported in this thesis.

Optical test.

An attempt has been made to examine the curvature of different parts of the crystal optically. For this optical test the strips T, M. and B were divided into seven nearly equal parts, (figure 17), so that the border regions of the adjacent subdivisions of the Hartmann test could be

FIGURE 18.
(Hartmann Test)

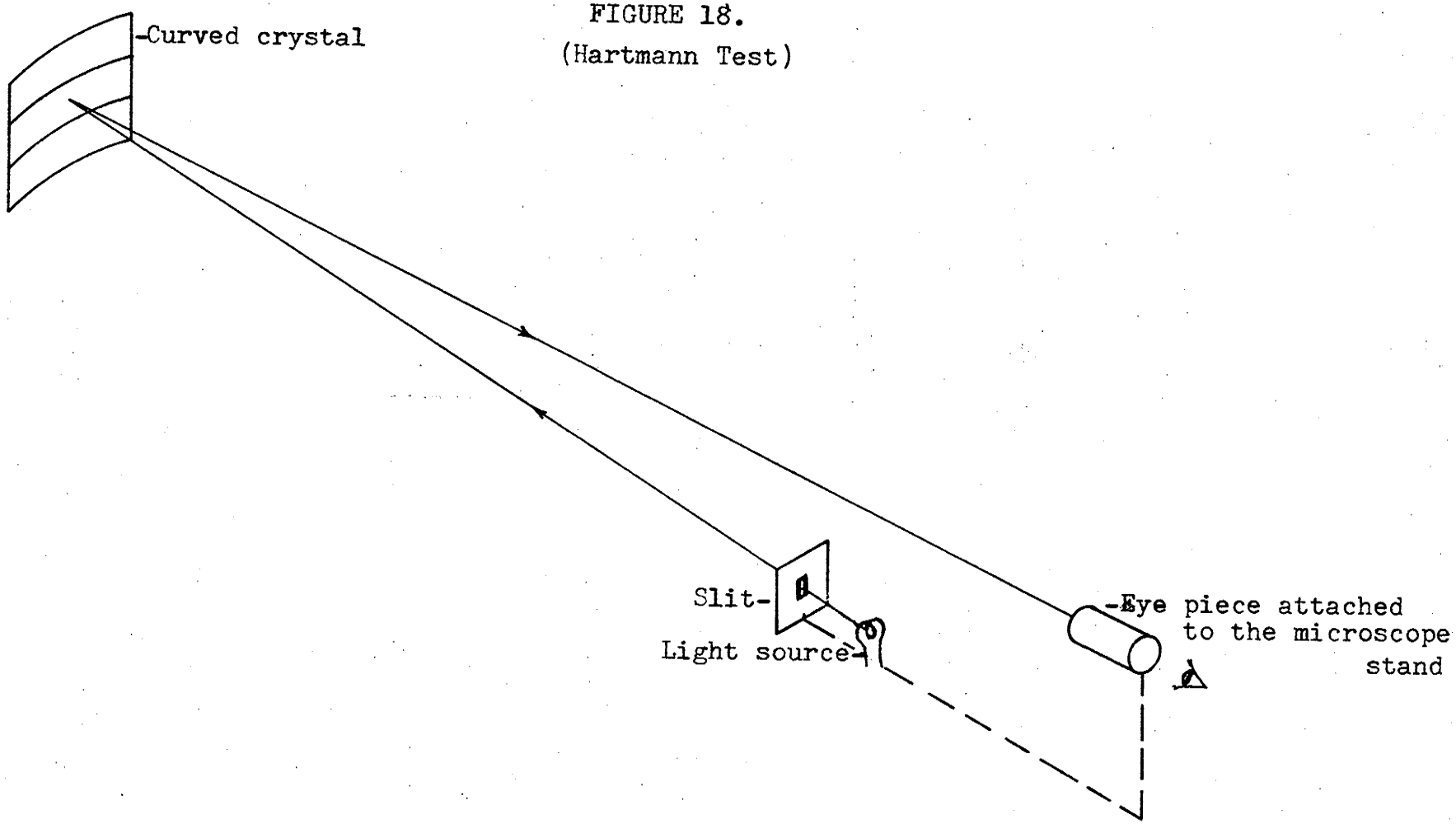

Optical arrangement for testing the curvature of the quartz crystal.

examined. These parts have been named as OT-1, ..., OT-7; OM-1, ..., OM-7 and OB-1, ..., OB-7. The source carriage was turned to the extreme left side. A table was placed on its four legs above the lower carriage and track of the diffraction spectrometer. The top of the table served as a horizontal platform of the proper height. An illuminated slit was the object for the curved crystal which functioned here as a cylindrical mirror. The slit was placed on the table top near the tract T (figure 1 and 2) at such a position that the image was formed right behind it. A microscope, with its eyepiece only, (objective removed), was placed behind the slit for observing the image. The eyepiece was moved forward or backward for focussing the image by hand only, as there was no precision arrangement available to move it in this direction. The object slit and the eyepiece were placed as close as possible, so as to get the image nearer to the centres of curvature of the crystal parts. Distance between the two (at the 'zero' position of the eyepiece) was about 25 cm. All these measurements had to be taken with an ordinary meter scale. The optical arrangement is shown in figure 18.

For each of the seven subapertures in each strip (T,M, & B) readings were taken for the lateral position and for the focal distance of the slit image. The focal distance is the distance by which eyepiece was moved forward or backward to focus the image. These distances have been measured from an arbitrary position of the eyepiece. The lateral positions also have been measured from an arbitrary zero.

A wide variation was observed in the lateral positions and focal distances. Variations of focal distances and lateral positions (of the slit image) with crystal subapertures are shown in figures 19 and 20.

In these figures, lateral positions are given in millimeter and focal distances are given in centimeter. Lateral positions of the images were

FIGURE 19. Hartmann Test Data.
Focal distances of the (optical) images obtained by reflection from 21 different parts of the curved crystal apertures.

Images for OT-6, OT-7, OM-6, OM-7, OB-2, OB-6 and OB-7 could not be focussed within the limited range of measurement, so their focal distances have not been shown.

(Focal distances are relative.)

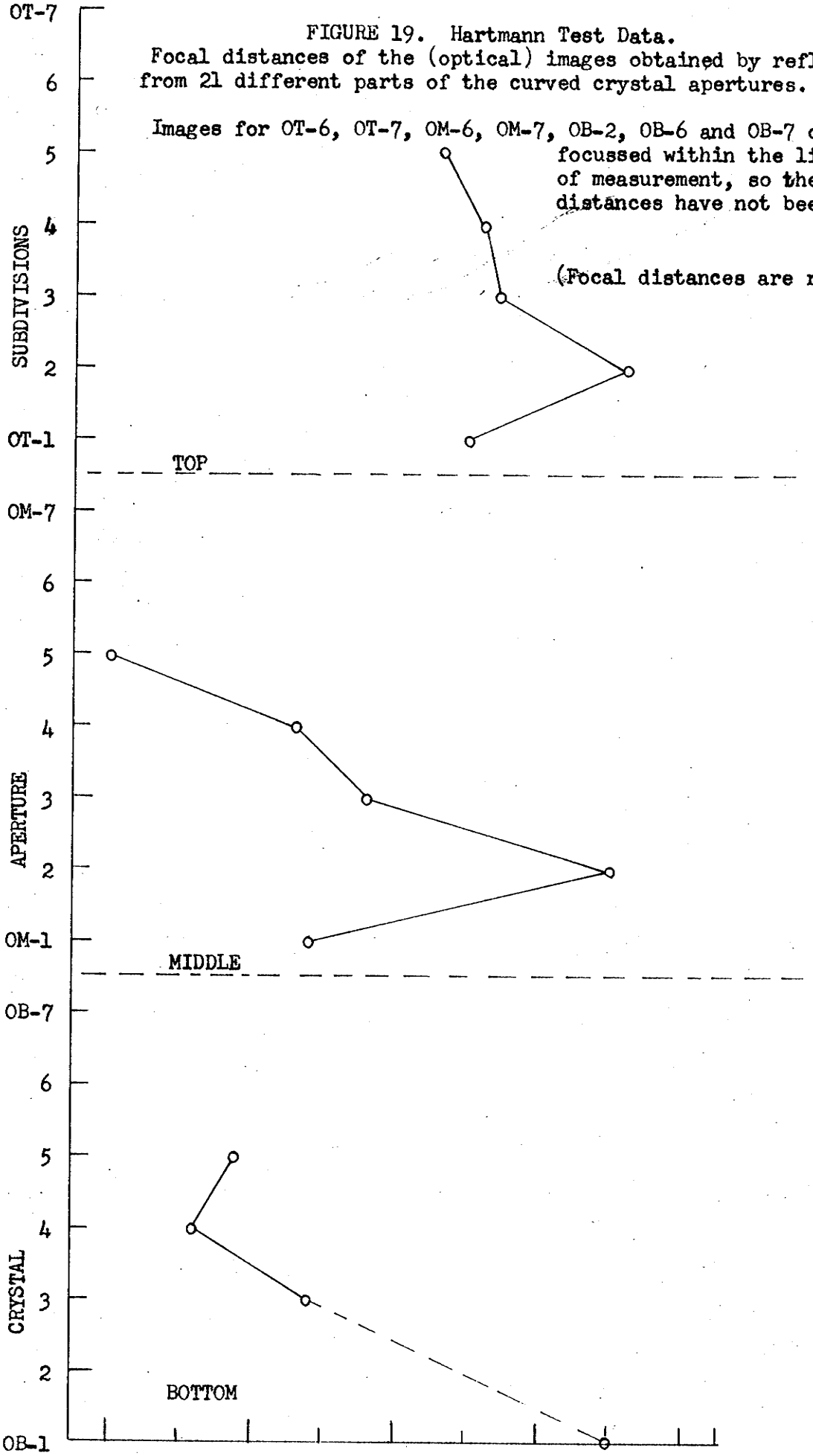

Distance by which the eye piece was removed from a fixed position to focus image.

FIGURE 20. Hartmann Test Data.

Lateral positions of the (optical) images obtained by reflection from 21 different parts of the curved crystal aperture.
o and + indicate the lateral positions of the two different images as observed through the eye-piece.

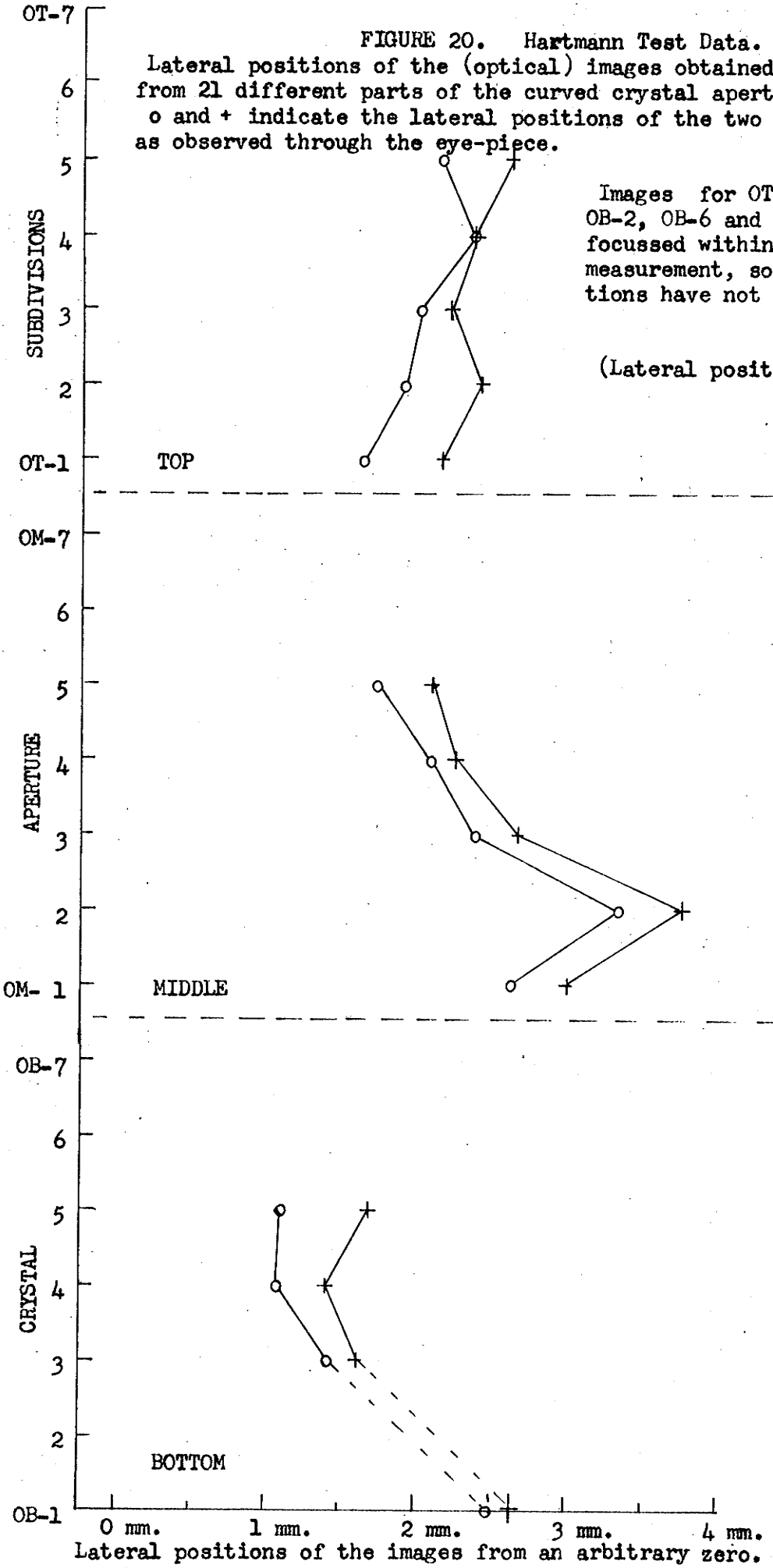

Images for OT-6, OT-7, OM-6, OM-7, OB-2, OB-6 and OB-7 could not be focussed within the limited range of measurement, so their lateral positions have not been shown.

(Lateral positions are relative.)

Lateral positions of the images from an arbitrary zero.

measured with the help of the scale and vernier arrangement attached to the microscope stand for lateral displacement measurements. So these measurements are quite accurate. Focal distances were measured with an ordinary scale judging with the naked eye. Therefore, these values may have an error of $\pm$ 2 or 3 mm.

Due to reflection from each subaperture, two images of the slit appeared. Their lateral positions are indicated by o and +, in figure 20. The reason for these double images is not clear. They may be due to reflection from the front and back surfaces of the bent crystal. This could have been ascertained by changing the reflectivity of the back surface with the help of water or grease. This was not done, because in doing so there was a possibility of scratching the crystal surface due to any dust being rubbed against it.

It was not always possible to focus both of these images at one and the same distance. Their focal distances varied within about 3 mm. As the difference in their focal distances was within the error limit of measurement, focal distances of the two images have not been shown separately.

Images due to reflection from some subapertures could not be focussed within the limited range of the table top. (This range was about 40 cm. behind the object slit.) So, no measurement of their focal distances was possible. Accurate determination of their lateral positions was also not possible, as these images were out of focus. So, their focal distances and lateral positions have not been shown in figures 19 and 20.

Measurement of such focal distances could have been done by making a longer platform (i.e. table top) to accomodate the microscope stand at any required distance from its arbitrary position and by moving the microscope stand foreward or backward with much care so as not to affect the

measurement of lateral positions of the images. However, as time was limited, it has not been possible to do so. Due to the same reason enough data for any positive inference about the curvature of the crystal could not be obtained.

Some relation can be observed between the optical test results and the gamma ray diffraction results.

Optical images for OT-6, OT-7, OM-6, OM-7, OB-2, OB-6, and OB-7 parts could not be focussed even at a distance of 40 cm. behind the object slit. (Images for other parts were fairly focussed within a distance of about 30 cm. behind the object slit.)

Diffraction curves (figures 8 and 9) show that T-5, M-5, B-5, B1½-½2 and B4½-½5 subdivisions have much less curvatures compared to other parts. T-5 and M-5 cover major portions of OT-6 and OT-7, and OM-6 and OM-7 respectively. This means, for these parts, diffraction results are supported by optical test results.

OB-2 part is somewhere in the region B1½-½2. Image for OB-2 could not be focussed within the limited range. This supports the diffraction result for B1½-½2 (i.e. this part is comparatively more flat.)

Focal distances of images for OB-6 and OB-7 are beyond range. Diffraction curve for B-5½ (the half portion of B-5 nearer to the clamping block side) is symmetrical, though broad and much less in peak intensity. (The width is 33 seconds of arc and peak counts are about 500 per minute.) Diffraction result for B4½-½5 show that this part has relatively less and uneven curvature. So, somewhere in between B-4 and B-5, the crystal is improperly bent.

Optical image for OB-1 part could be focussed. Diffraction curve for B½1 (the half portion of B-1 nearer to the clamping block) is quite symmetrical. The width is 30.46 seconds of arc and the peak count is

about 3,000 per minute. So, optical test and diffraction result show that $B\frac{1}{2}1$ part has a proper curvature.

Optical images for other parts of the crystal could be focussed within about 4 cm. Diffraction curves for such parts are better in shape.

Variations in focal distances and lateral positions of the optical images (figure 19 and 20) indicate that centres of curvature of different parts of the crystal are distributed in the directions of X and Y axes of a horizontal plane. No significant variation in the vertical (Z axis) direction has been observed.

CHAPTER IV

RELATIVE INTENSITY MEASUREMENT OF IRIDIUM - 192 GAMMA RAYS

Introduction.

The (n, γ) reaction in Iridium - 191 gives rise to triple isomers[9] of Iridium - 192: A long lived ($T_{\frac{1}{2}} > 5$ years) isomer Iridium - 192_{m_1} decaying by a 161 kev isomeric transition to the 74.3 day ground state, 1.45 minute isomer Iridium - 192_{m_2} decaying mainly by a 58 kev isomeric transition to the 74.3 day ground state and 74.3 day isomer Iridium - 192 g.

The 74.3 day Ir-192 g decays by beta emission (95.6%) to Pt - 192 and by orbital electron capture (4.4%) to Os - 192[10].

The resulting gamma rays from the excited states of Pt - 192 and Os - 192 have been extensively studied [10-19]. In this study, curved crystal spectroscopy[10, 12, 13, 14] has player a major role along with internal conversion [15, 16] and external (photoelectric) conversion[10,17,20] spectroscopies.

Recently (1963) B. Lindstroem and I. Marklund[10] have re-determined gamma energies of Ir - 192 relative to the well known $K^{\alpha}1$ x-ray line of Tungsten (208.573 ± 0.004 X-units) with a 2 meter curved quartz crystal (thickness 1.5 mm.) transmission spectrometer of the DuMond type, with a fixed source and a movable crystal and detector and also by a double focussing beta spectrometer using photo-conversion method.

Though energies of gamma rays resulting from the decay of Ir - 192 are well established through the works of different research workers,[10,11 12, 14-17,] there appear to be some disagreements over their relative intensities. This can be observed from table IV, which shows the values

of relative intensities quoted by different researchers in this field.

From table IV, it may be noted that, while the relative intensities for lines close to the 316.5 kev line, with respect to which all relative intensities are normalized, are in good agreement, values for many other lines are not. There are some outstanding conflicts between values quoted by different workers, even following the same method of determination (i.e. either the crystal diffraction method, or the Photo-conversion method).

For example, while data for the 136, 201 and 206 kev lines in column 4 are about twice the respective data in column 2 and 5; for 468, 484.6, 589, 605 and 612 kev's, data in column 5 are 2 times, $3\frac{1}{2}$ times, $6\frac{1}{2}$ times, 10 times and 17 times greater than the respective values in Column 4.

Similar disagreement can be observed if we compare column 6 with column 5. For 136 kev line, data in column 6 is about 19 times greater than the data in column 5, for 201 and 283 kev lines, data in column 6 is twice the data in column 5, while for 375 kev gamma energy line, the data in column 5 is about three times greater than the data in column 6.

On the whole, there is little agreement between the values in different columns. Column 7 shows fair agreement with column 2 and 8, but does not give values for low energy or low intensity lines.

The above discussion shows that, there is scope for much work in this aspect of the decay of Ir - 192, and so it was decided to make an attempt to remeasure the relative gamma ray intensities for this isotope.

The source.

For determining relative intensities, a strong source (about 12 curies) of Ir - 192 was used. This was obtained by irradiating an iridium strip 1.4 inches in length, 0.013 inches in breadth and 0.002 inches

in thickness in a flux of 2×10^{14} neutrons per $cm.^2 \times sec.$

Procedure (Experimental).

For each setting of the curved crystal spectrometer, intensity of the reflected beam was measured by determining the number of counts registered by the scalar per minute. Minimum counting period was five minutes. The counting periods were long (ten minutes to an hour) in the regions of the spectrum where the counting rate was low. The counting periods were short (up to ten minutes) in the regions where high counting rates gave sufficiently good statistics.

Background for each spectrum was determined in the following way.

The spectrometer was set to the lower or higher energy end of the spectral line profile. The position of the spectrometer was such that, a fractional dial turn could make just a perceptible change in the counting rate above the lowest counting rate.

Keeping the spectrometer at this position, the pulse height selector voltage (V_{PHS}) level of the single channel analyser was changed by a step of 0.25 or 0.5 volts (and the gate width accordingly) within the limited range for the particular line profile. Counting rate was noted for each setting of the single channel analyser. These settings were later changed into equivalent dial turns. (While taking counts for a line profile, V_{PHS} and gate width was varied according to the number of dial turns, so that the pulse height selector gate could admit only the pulses which had the same energy as the gamma rays reflected by the curved crystal according to the Bragg relation. By reversing the process of calculation, equivalent number of dial turns for V_{PHS} was obtained.) So, for each of such equivalent number of dial turns,

two separate counting rates were obtained; one, with the spectrometer on the lower energy side, and the other, with the spectrometer on the higher energy side. Mean of these two counting rates were plotted against the dial turns on the line profile graph. By joining these points, the background level was determined for the particular line profile.

After taking the precautions described earlier, in chapter II, background counts are mainly due to some gamma rays of nearer energy, which succeed in passing through the quartz crystal and baffle system without being diffracted or absorbed. So by changing the discriminator bias level, and keeping the spectrometer on lower or higher energy end of the photopeak as described, a scintillation spectrum of the background due to these undiffracted an unabsorbed gamma rays is obtained.

All these counts were extrapolated (i.e. corrected for radioactive decay) to a zero day (October 10, 1964) counts as if the counts for the whole spectrum were taken on that day. For this the half life of Ir - 192 was taken as 74.3 days. As this is quite a long half life, correction for decay to the hour was not considered.

Spectra of Ir - 192 from 613 kev to 136 kev lines were obtained on reflection from one particular side (left side to an observer facing crystal from "zero" position) of the transverse crystal planes as this side line profiles were more symmetrical compared to the other side line pro-

TABLE V

Variation in planimeter readings for a standard area-- 10,000 unit squares (sq. mm.) of a metric graph paper.
155.0
154.0
154.0
155.2
153.0
154.5
154.0
155.0
153.5
154.2
Average: 154.2

Determination of the Normalized Photopeak area or Uncorrected Intensity of the Gamma Energy Line: An Example.

	Planimeter Readings for		
	206 kev line profile (background deleted)	308.5 kev line profile (background deleted)	316.5 kev line profile (background deleted)
	472.5	588.0	709.0
	473.5	586.0	710.0
	473.6	586.5	708.0
	474.5	586.0	708.6
	476.5	587.5	709.2
Average:	474.1	586.8	709.0

All gamma ray profiles were drawn on metric graph paper. The horizontal scale (representing the dial reading) was the same for all profiles. The vertical scale had to be changed from profile to profile.

Therefore, to determine the relative area, the planimeter reading has to be multiplied by the respective vertical scale unit. For 206, 308.5 and 316.5 kev line profiles, the vertical scale units are 20 counts, 50 counts and 100 counts per minute respectively. Taking the photopeak area for 316.5 kev line as 1,000, the photopeak area for 206 and 308.5 kev lines are:

$$\frac{20 \times 474.1 \times 1,000}{100 \times 709.0} = 133.7$$

and $\frac{50 \times 586.8 \times 1,000}{100 \times 709.0} = 413.7$ respectively.

files. (This has been discussed in chapter III.) This symmetrical nature of the line profiles has made it possible to determine the exact shape of the curves for each line, in cases of overlapping profiles. (Figure 11.)

Areas of the different line profiles (after deleting the respective backgrounds) were measured with the help of a planimeter. For each profile, several measurements were taken by changing the position of the planimeter centre needle, so as to see if there is any error due to the slipping of the planimeter dial. Average of the readings, which agree well, was taken as the representative of the individual areas. (Samples of some planimeter data have been displayed in table V.) Values of all these areas were normalized with respect to the area of the 316.5 kev line profile taken as 1,000. Determination of the areas of certain line profiles close in energy (e.g. 589, 605, and 613 kev, and 468 and 485 kev lines) posed some difficulty due to overlapping. This was solved from the symmetry nature of the curves, as shown in figure 11.

Procedure (analytical).

In calculating relative gamma ray intensities by the crystal diffraction method, the following effects need to be considered: (i) The efficiency of the scintillation spectrometer used as a detector of the gamma radiation, (ii) self absorption in the source, and the (iii) reflection efficiency of the curved crystal.

(i) Scintillation efficiency

The total detection efficienty of a scintillation spectrometer is a product of two factors: the detection efficiency of the scintillating crystal 'e' and the photopeak efficiency or photo-fraction Fp = Np/Nt, where Np is the number of counts per second in the full energy photopeak (i.e. the area of the line profiles), and Nt is the total number of counts

TABLE VI

(Taken from the book
'Theory and Practice of Scintillation Counting'
by J. B. Birks, Pergamon Press, 1964.)

Values of parameters of the empirical formula for the photofraction, $Fp = A - B.\exp.(-C.\sqrt{d.r})$
d is the thickness and r is the radius of the scintillating crystal.

Gamma ray energy in Mev	Values of Parameters		
E	A	B	C(Cm^{-1})
0.279	0.973	0.514	0.658
0.661	0.940	0.841	0.219
1.170	0.980	0.934	0.124
1.330	0.985	0.942	0.210

FIGURE 21.

Photopeak efficiency (i.e. photo-fraction F_p) of the $4\frac{1}{2}$ inches by $\frac{1}{2}$ inch scintillating crystal (NaI(Tl)) as a function of energy.

Detection efficiency, e of the $\frac{1}{2}$ inch thick scintillating crystal (NaI(Tl)) as a function of energy.

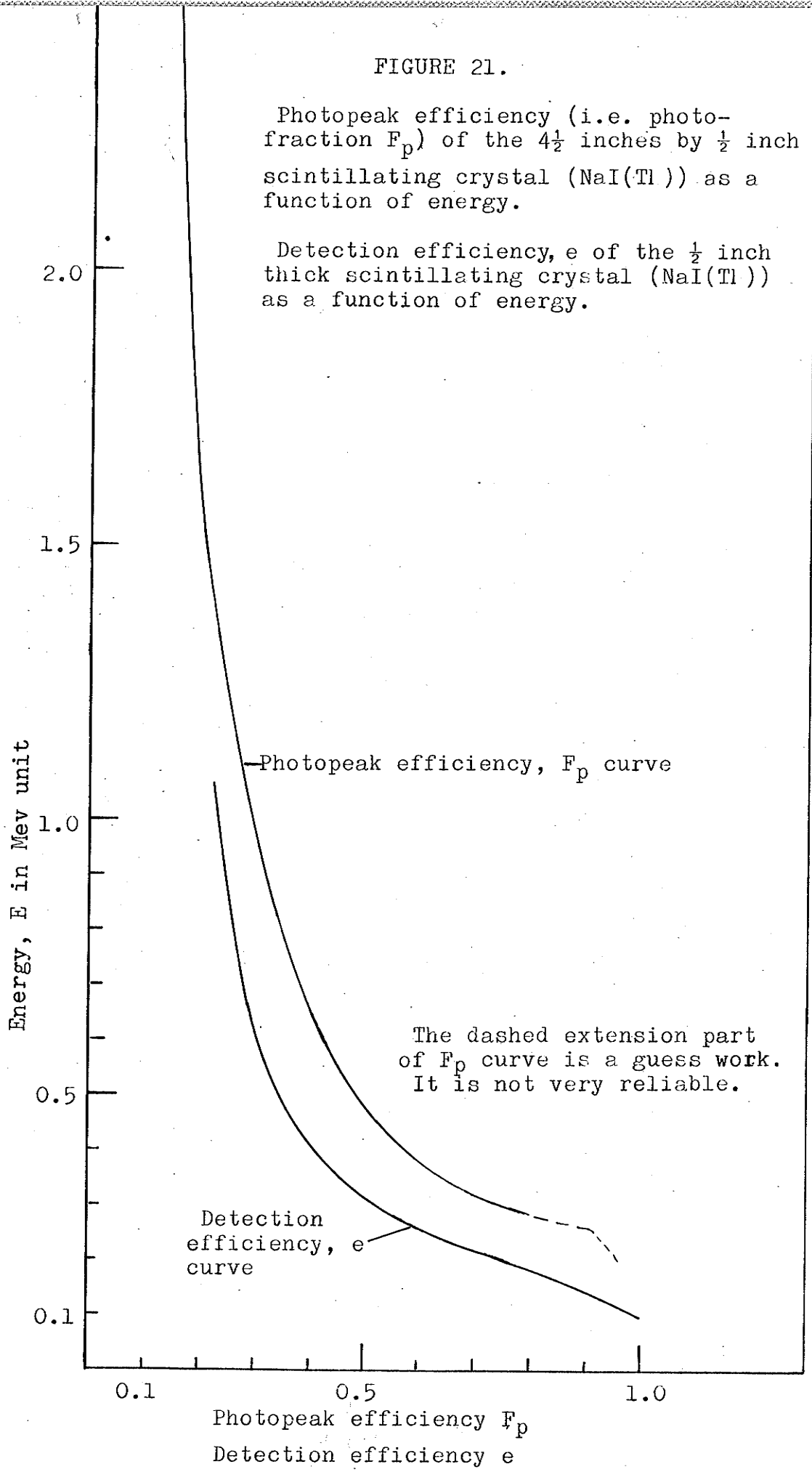

FIGURE 22.

Self-absorption correction ($a = \frac{I}{Io}$) for the source Ir-192 as a function of energy.

(I is the intensity after self absorption and Io is the intensity without absorption.)

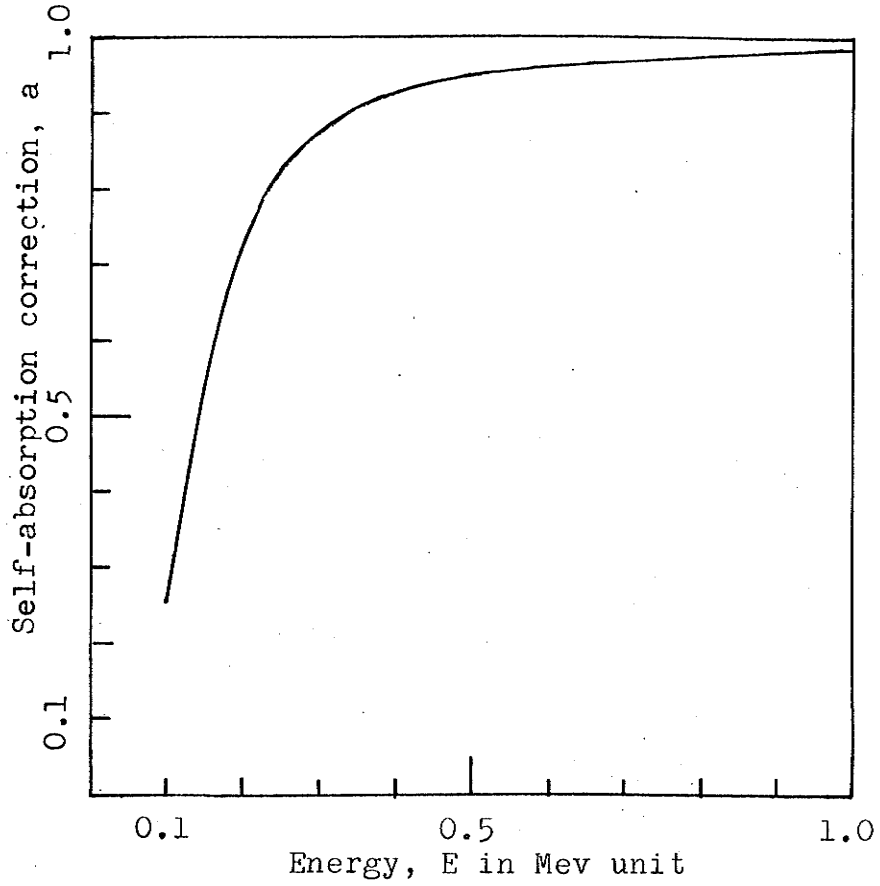

per second (corrected for background) over the whole scintillation spectrum, each of which is a complicated function of energy. These functions have been computed for various crystal sizes. However, the crystal used here being of an unusual size ($\frac{1}{2}$" by $4\frac{1}{2}$"), values for these functions could not be found from the literature. They were obtained in the following way.

For a collimated beam of gamma rays, incident normally (which is the case in our experimental arrangement) on a scintillator of a thickness d and radius r, Fp can be obtained from the empirical formula:

$$Fp = A - B \exp \left(-C \cdot \sqrt{dr} \right)$$

for energies in the range from 0.279 to 1.33 Mev, where A, B, and C are energy dependent parameters having the values listed in the table VI. This empirical formula and table VI have been obtained from the book - "Theory and Practice of Scintillation counting" by J. B. Birks, Pergamon Press (1964).

A graph (figure 21) E versus Fp was drawn by calculating the values of Fp corresponding to the four different energies as given in table VI. Values of Fp for different gamma energies were read from the graph. Values for 206, 201 and 136 kev's could not be obtained correctly as the above relation is not valid for these energies.

Detection efficiency e was determined from the following well known formula:

$$e = 1 - \exp \left(-\mu d \right)$$

where μ is the total absorption coefficient which is energy dependent. Values for μ were obtained from Mott and Suttons' work[25]. The value of e as a function of E (energy) is shown in figure 21.

(ii) Self absorption of the source

For self absorption, consideration was taken as follows:

The atomic number of irridium is 77, so the source material is quite

absorbing for gamma and x-rays. The Ir source is contained in a very thin ($\ll$1 mm. in thickness) aluminum foil. The scintillation crystal (which detects the gamma rays) is also contained in a thin aluminum casing (less than a millimeter in thickness). As the atomic number of aluminum is 13, absorption due to it is negligible compared to the source itself.

Let us assume that the source is a parallelepiped with gamma rays coming out in one direction through the front surface. As the source itself has finite depth, gamma rays coming from the material at the back must pass through the source material in front and would be absorbed. Intensity of these gamma rays will be reduced. This reduction in intensity depends on the gamma energy. If dI is the intensity of gamma rays from an element dx at a distance x from the front surface, then $dI = k.\,dx.\,\exp(-ux)$, where k is the intensity per unit depth of the source, u is the linear absorption coefficient of the source and x ranges from 0 to b, where b is the depth of the source material. For the present source the value of b is 0.013 inches.

If there is no absorption at all, then

$$Io = kb$$

Therefore, $$I = \int_0^b k.\exp(-ux)dx = (Io/b)\int_0^b \exp(-ux)dx$$
$$= (Io/bu)\,(1 - \exp(-bu))$$

or, $$\frac{I}{Io} = (1/bu)\,(1 - \exp(-bu))$$

This formula can be written as follows: $\frac{I}{Io} = (1/b\varrho.u/\varrho)\,(1 - \exp(-b\varrho.\,u/\varrho))$ where ϱ is the density of the absorbing material. Values for u or u/ϱ could not be found for irridium. However, for platinum (which is very close in atomic number and density to irridium) values for u/ϱ are given in Kai Siegbahn's alpha, beta and gamma ray spectroscopy, Volume I (1965). Using these values, a graph E versus I/Io was drawn (figure 22). Values for different gamma lines were taken from this graph.

(iii) Crystal Reflectivity

The reflection properties of elastically bent transmission quartz crystals (310 plane) have been studied by several workers. Bergvall[26] has given the equation for reflection coefficient R as, $R = \text{const. } E^{-1.99 \pm 0.05}$ and Edward et al[22] have given the relation $R = \text{const. } E^{-1.987 \pm 0.022}$. These two equations are in close agreement and show that the value of the exponent is nearly -2. For the present calculation, as a first approximation, the value of the exponent has been taken as -2. (Reflection coefficient of the present crystal has been determined and the value of the exponent has been found to be -1.95. This will be discussed later.)

Lind et al[29] have studied the reflection coefficient for the (310) planes of quartz as a function of wavelength for curved quartz plates over the large range from 700 x-units to 9 x-units and have found that the reflection coefficient is proportional to the square of the wavelength i.e. $R = \text{const. } \lambda^2$. On the contrary, their tests for unstressed quartz plates show that the reflection coeffieient falls off with diminishing wavelength, λ, even less rapidly than the first power of λ, (roughly as $\lambda^{\frac{1}{2}}$ in fact). These results are interesting from the point of view of purely empirical facts. As remarked by them, their theoretical interpretation is less clear, however, since no "dynamical theory" of x-ray reflection in elastically curved crystals has yet been worked out either for the mosaic or perfect crystal cases.

Analysed data.

Values of the absorption correction $a = I/I_o$, detection efficiency of the scintillating crystal e, photopeak efficiency of the scintillating crystal (i.e. photofraction) Fp, reflection coefficient $R = (316.5)^2 . E^{-2}$, uncorrected intensity, I_u (i.e. photopeak area Ap) normalized with respect to that of 316.5 kev line taken as 1,000.00 and corrected normalized inten-

TABLE VII

Spectral energy line in kev unit	Uncorrected normalized intensity (i.e. normalized photopeak area)	Correction for self-absorption of the source	Detection efficiency of the scintillating crystal	Photopeak efficiency of the scintillating crystal	Reflection coefficient of the curved quartz crystal	Corrected normalized intensity
E	I_u	$a = \frac{I}{I_o}$	e	F_p	R	I_c
136.3	2.1	0.48	0.91		5.39	
201.3	24.3	0.75	0.75	0.96 *	2.47	5.8 *
205.8	133.7	0.76	0.73	0.96 *	2.37	33.3 *
283.4	5.4	0.87	0.55	0.81	1.25	3.4
295.9	405.6	0.88	0.53	0.76	1.15	314.4
308.5	413.7	0.89	0.51	0.72	1.05	376.1
316.5	1,000.0	0.90	0.50	0.70	1.00	1,000.0
374.7	4.5	0.92	0.43	0.60	0.71	8.2
416.6	3.8	0.93	0.39	0.55	0.58	10.1
467.9	148.9	0.95	0.36	0.50	0.46	585.9
484.6	10.9	0.95	0.35	0.49	0.43	48.7
588.9	6.1	0.96	0.31	0.43	0.29	51.3
604.7	11.6	0.96	0.31	0.42	0.27	106.7
612.9	6.0	0.96	0.30	0.42	0.27	57.4

* Doubtful values.

sity I_c, where I_c = Iu/a.e. Fp.R, corresponding to the different gamma energies, E, are given in table VII.

As relative intensities are normalized with respect to the 316.5 kev line intensity, the constant for reflection coefficient R is cancelled out in calculations. So this constant has been taken as $(316.5)^2$ for convenience of calculations.

Discussion.

In the present work errors in determination of relative photopeak areas (i.e. uncorrected normalized intensities Iu) have been found to be $\leqslant 1\%$. These errors have been quoted in table VIII. Errors due to other factors, for which reliance have been made on others' work, could not be estimated. So no attempt has been made to quote errors for the present relative intensity values. (Lindstroem and Marklund[10] have reported an over all error of 6 to 9% in determination of relative intensities by curved crystal diffraction method due to different factors. Their error in determination of photopeak areas for all lines is less than 2%[10].) The relative intensities are given in table IV, column 1, along with the values of all earlier determinations for comparison.

From table IV it is apparent that determination of relative intensities for 283, 375, or 416.6 kev lines by curved crystal diffraction method has not been reported earlier. Reason for this is not clearly understood. A possible reason may be that the sources used by earlier workers were not as strong as the present one. Lindstroem and Marklund[10] used a source of 1.2 curies in strength and Sumbaev[14] used a source of 1 curie in strength. (Strength of the source used by Muller et al[11] is not known.) Even then, the relative intensities of the 375 and 416.6 kev lines does not appear to be too weak to escape notice.

Further, for these three lines, values reported by photo conversion

TABLE IV

Relative Intensities of Iridium - 192 gamma rays

as reported by different research workers.

By Crystal Diffraction Method				By Photo-Conversion Method				
Present	Marklund and Lindstroem[10]	Sumbaev[14]	Muller[11#]	Baggerly[12]	Johns and Nablo[17]	Hamilton et al[20]	Marklund and Lindstroem[10]	Average of columns 2 and 8 as reported by Marklund and Lindstroem[10]
	2.7 ± .5		4	1.9	34		4 ± 2	2.7 ± 0.5
6	5.6 ± .6		10	4.6	10		45 ± 7	5.6 ± 0.6
33	37 ± 4	50	75	39	45			38 ± 4
3.4				6	13		4 ± 2	4 ± 2
314	370 ± 25	365 ± 37	380	360 ± 70	340 ± 70	375 ± 20	350 ± 30	360 ± 20
376	360 ± 25	370 ± 37	370	350 ± 70	360 ± 70	395 ± 30	380 ± 30	370 ± 20
1000	1000	1000	1000	1000	1000 ± 200	1000	1000	1000
8				19	6.5		6 ± 2	6 ± 2
10				16			3	3
586	630 ± 60	610 ± 70	300	640 ± 130	740 ± 150	660 ± 70	580 ± 50	600 ± 40
49	42 ± 4	57	11	39	68		38 ± 5	40 ± 4
51	52 ± 5	64 ± 6	11	71 ± 14	83 ± 17	49 ± 5	45 ± 6	49 ± 5
107	110 ± 10	120 ± 12	14	140 ± 30	130 ± 26	96 ± 10	100 ± 11	105 ± 7
57	75 ± 7	89 ± 9	5	84 ± 17	100 ± 20	60 ± 10	65 ± 8	70 ± 5
1	2	3	4	5	6	7	8	9

reservation is made that lines widely spaced in energy cannot be accurately compared.

rs quoted in columns 3, 5, 6 and 7 have been obtained from Arkiv för Fysik, 22 (1962) 485, (Hamilton et al).

methods are not in agreement.

For the 283 kev line, the present value agrees fairly well with the data in column 8, for the 375 kev line, agreement can be observed with the data in column 6 and 8, whereas for 416.6 kev line, the present value is in disagreement with any other data (Baggerly's 16, Lindstroem's (3).

Present values for the 201, 589 and 605 kev lines agree well with the respective values in column 2 and the 613 kev line agrees with column 7. Values quoted in column 7 for 589 and 605 kev lines are also in fair agreement with the respective present values.

Present values for the 206 kev and 484 kev lines are in fair agreement with the respective data in column 2 and the 468 kev line is in fair agreement with data in column 2 and 3. The value for 469 kev line is in good agreement with data in column 8.

For lines close in energy to the 316.5 kev line, there is fairly good agreement in relative intensity values given in columns 2 to 6. This is expected, because relative intensities are normalized with respect to that of 316.5 kev. While the present value for the 308.5 kev line agrees very well with others' data, the value for the 296 kev line is low by 11% to 20%. (Measurements for this line have been repeated, but no error could be observed.)

'Fp' for the 136 kev line could not be obtained, so no attempt has been made to calculate its relative intensity with the knowledge of scintillation efficiency. However, the relative intensity (value 0.11) for this line has been obtained from the knowledge of over all efficiency of the spectrometer. This is in complete disagreement with the values of other workers. This will be discussed later.

Marklund and Lindstroem[10] have determined the relative intensities

for Ir - 192 gamma rays by the two different methods. Average of their values, as given by them, are reported in column 9. On the whole, the present values are in fair agreement (within 2 to 15%) with the respective values in column 9, except for the 613 kev line, where the present value differs by about 22%, for the 375 kev line, where the difference is 27% and for the 416.6 kev line, where the difference is more than 70%.

From table IV it can be observed that, Muller's values (column 4), except for the 295 and 308.5 kev lines, do not agree with any other's values. Column 7 and 8 are in fairly good agreement, except for the 468 kev line, where the value in column 7 is nearer to the value in column 2. Values in columns 5 and 6 are not in much agreement, nor do these agree with other columns. As a possible reason for this disagreement, Hamilton et al[20] have pointed out that, the disagreement of the results in columns 5 and 6 with column 7, (all of which have been determined by photo conversion method), may easily arise from the correction for the photo electron angular distributions. They have also observed[28] certain differences in 'f' factor calculations in the very transitions studied. According to them, at the time of studies reported in columns 5 and 6 very little was known about these angular functions. So relative discrepancies might easily be present in Baggerly's and John's (i.e. columns 5 and 6) data.

Determination of efficiency rule.

An attempt has been made to determine the over all efficiency of the present spectrometer (along with the scintillation spectrometer as one unit). For this purpose, in view of the above discussion, values in columns 3, 7 and 9 only were taken into consideration. (As mentioned earlier, column 9 is the average of columns 2 and 8 reported by the same group or workers, Lindstroem and Marklund[10], who have observed that,

TABLE VIII

Spectral Energy line in kev unit	Normalized photopeak area or uncorrected intensity	Weighted average of intensities determined by earlier workers	Ratio $\frac{E_o}{E}$ (E_o=316.5 kev)	Ratio $\frac{I_u}{I_w}$
E	I_u	I_w		
136.3	2.1 ± 0.02	2.7 ± 0.5	2.32	0.77 ± 0.14
201	24.3 ± 0.08	5.6 ± 0.6	1.57	4.34 ± 0.46
206	133.7 ± 0.23	38 ± 4	1.54	3.53 ± 0.35
283.4	5.4 ± 0.04	4 ± 2	1.12	1.34 ± 0.67
296	405.6 ± 0.49	367 ± 21	1.07	1.11 ± 0.06
308.5	413.7 ± 0.50	378.3 ± 27	1.03	1.09 ± 0.08
316.5	1,000	1,000	1.00	1.00 ± 0.00
375	4.5 ± 0.03	6 ± 2	0.85	0.74 ± 0.20
416.6	3.8 ± 0.03		0.76	
468	148.9 ± 0.25	617.5 ± 55	0.68	0.24 ± 0.02
484.6	10.9 ± 0.05	40 ± 4	0.65	0.27 ± 0.03
589	6.1 ± 0.04	49 ± 5	0.54	0.12 ± 0.01
605	11.6 ± 0.06	106.5 ± 9	0.52	0.11 ± 0.01
613	6.0 ± 0.04	66.7 ± 7	0.52	0.09 ± 0.00

FIGURE 23.

Determination of the empirical efficiency rule for the 1.2 meter curved crystal spectrometer operated in tandem with the scintillation spectrometer as one unit. (Empirical rule for relative intensity determination.)

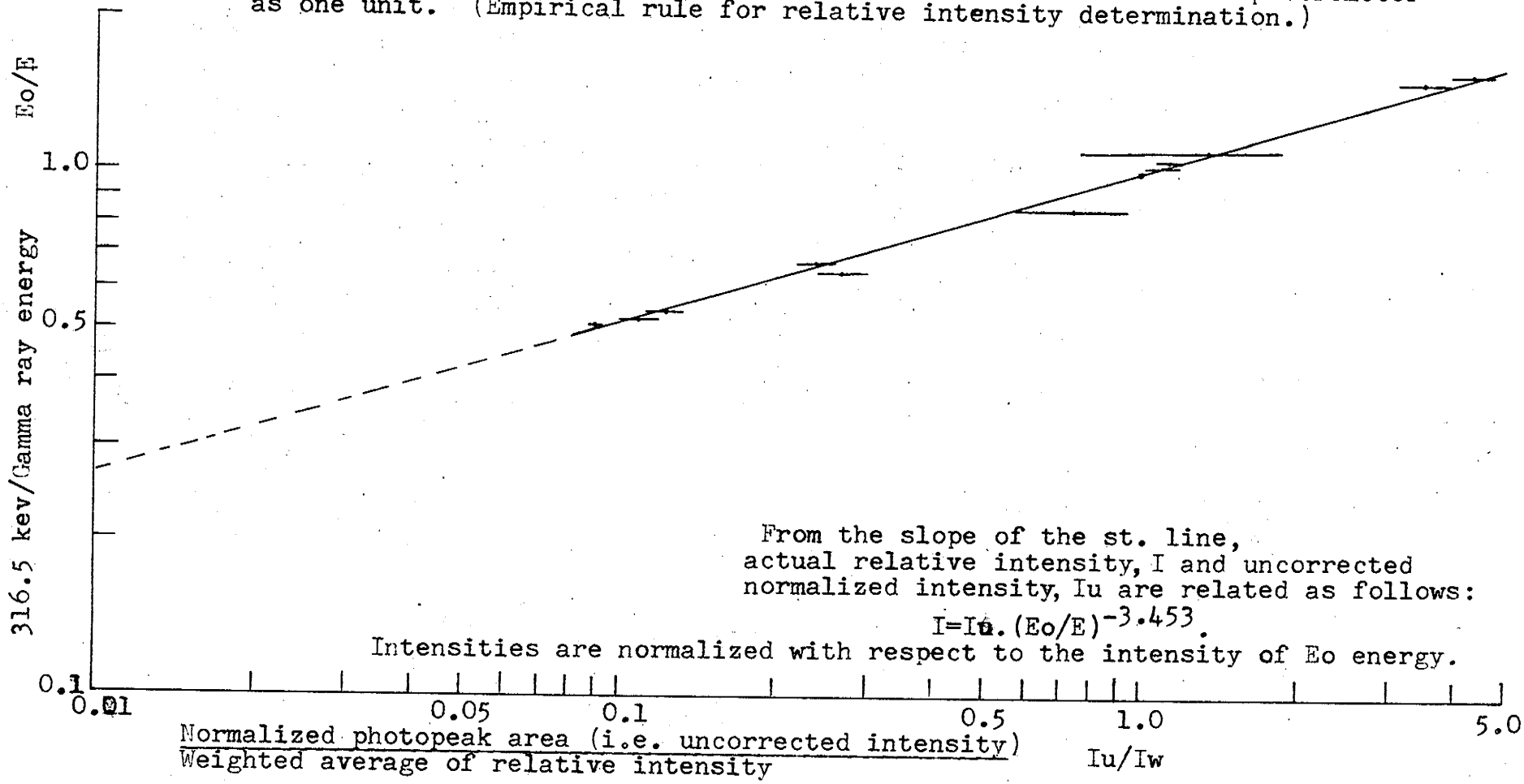

the crystal diffraction intensity determinations (column 2) of the gamma rays above 400 kev are somewhat higher than the photo conversion determinations (column 8). But, as their intensity determinations do not show any systematic deviation outside the experimental errors, they have quoted the weighted means (column 9) from the two methods.)

Giving weights inversely proportional to the errors quoted, the weighted average of the values (which are fairly close) for each line were taken into consideration for the over all efficiency determination.

For the lines 206, 484, 589 and 613 kev, values in column 3 are much higher than the values in column 9. As column 9 reports averages of values by two different methods, it is justified in relying more on these values. So for these lines, values in column 3 were discarded for averaging purposes. These weighted average values Iw are given in table VIII.

From Table VIII, values for (Eo/E) (where Eo is 316.5 kev) were plotted against values for Iu/Iw on a log-log graph (figure 23). A best fit straight line was drawn through these points with the consideration that it must pass through the point (1,1) (i.e. the representative point of the 316.5 kev line with respect to which intensities are normalized). From the slope of the straight line the following relation was obtained:

$$\ln (Iu/Iw) = 3.453 \ln (Eo/E)$$

or

$$Iu/Iw = (Eo/E)^{3.453}$$

From this efficiency rule for the spectrometer, it can be inferred that, actual relative intensity = $Iu.(Eo/E)^{-3.453}$.

With the help of this relation, relative intensity was calculated for each line. Values agree very well (within limit) with the values al-

TABLE IX

Spectral energy line in kev unit	Relative intensity obtained by efficiency rule	Relative intensity obtained by analytical procedure	Relative intensity not corrected for the reflectivity of the curved crystal	Ratio: $\frac{I_{Ru}}{I_e}$
E	I_e	I_c	I_{Ru}	
136.3	0.1			
201	5.1	5.8	14.3	2.80
206	30.2	33.3	78.7	2.60
283.4	3.7	3.4	4.3	1.18
296	321.1	314.4	360.0	1.12
308.5	377.5	376.1	396.1	1.05
316.5	1,000.0	1,000.0	1,000.0	1.00
375	8.0	8.2	5.8	0.73
416.6	9.7	10.1	5.8	0.60
468	575.8	585.9	267.8	0.47
484.6	47.4	48.7	20.7	0.44
589.0	51.8	51.3	14.8	0.29
605	109.0	106.7	29.2	0.27
613	58.6	57.4	15.3	0.26
Column: 1	2	3	4	5

ready obtained (as reported in table IV). Both the values are quoted in table IX for comparison (column 1 and 2). This agreement ascertains the validity of the efficiency rule. This also reflects on the accuracy of the present values compared to the more reliable values of earlier determinations.

The value (0.1) obtained for the 136 kev line by efficiency rule is in complete disagreement with any of the values obtained earlier for this line. Values reported by other workers for this line vary from 1.9 (Baggerly[12]) to 34 (Johns and Nablo[17]). The relative intensity for this line could not be obtained through analytical procedure, as the F_p value for 136 kev is not known. So, no conclusion can be drawn about its relative intensity. However, the value 0.1 does not seem to be reasonable. Therefore, the validity of the efficiency rule for 136 kev is doubtful. This rule appears to be valid within the energy range of 200 to about 600 kev. The upper limit may be greater than 600 kev, but, for the present, there is no opportunity to ascertain it.

Conclusion.

From the studies made here it can be concluded that, curved crystal diffraction spectrometry is quite a powerful tool for determining relative intensities of gamma transitions provided the source is strong enough.

With the help of the empirical efficiency rule, relative intensity of any gamma transition within the energy range of 200 to 600 kev can be directly determined with this whole instrumental assembly as one unit, though, before doing so, it will be useful to verify this rule with the help of some standard sources.

FIGURE 24.

Determination of the REFLECTION COEFFICIENT of the 310 plane of quartz crystal (curved).

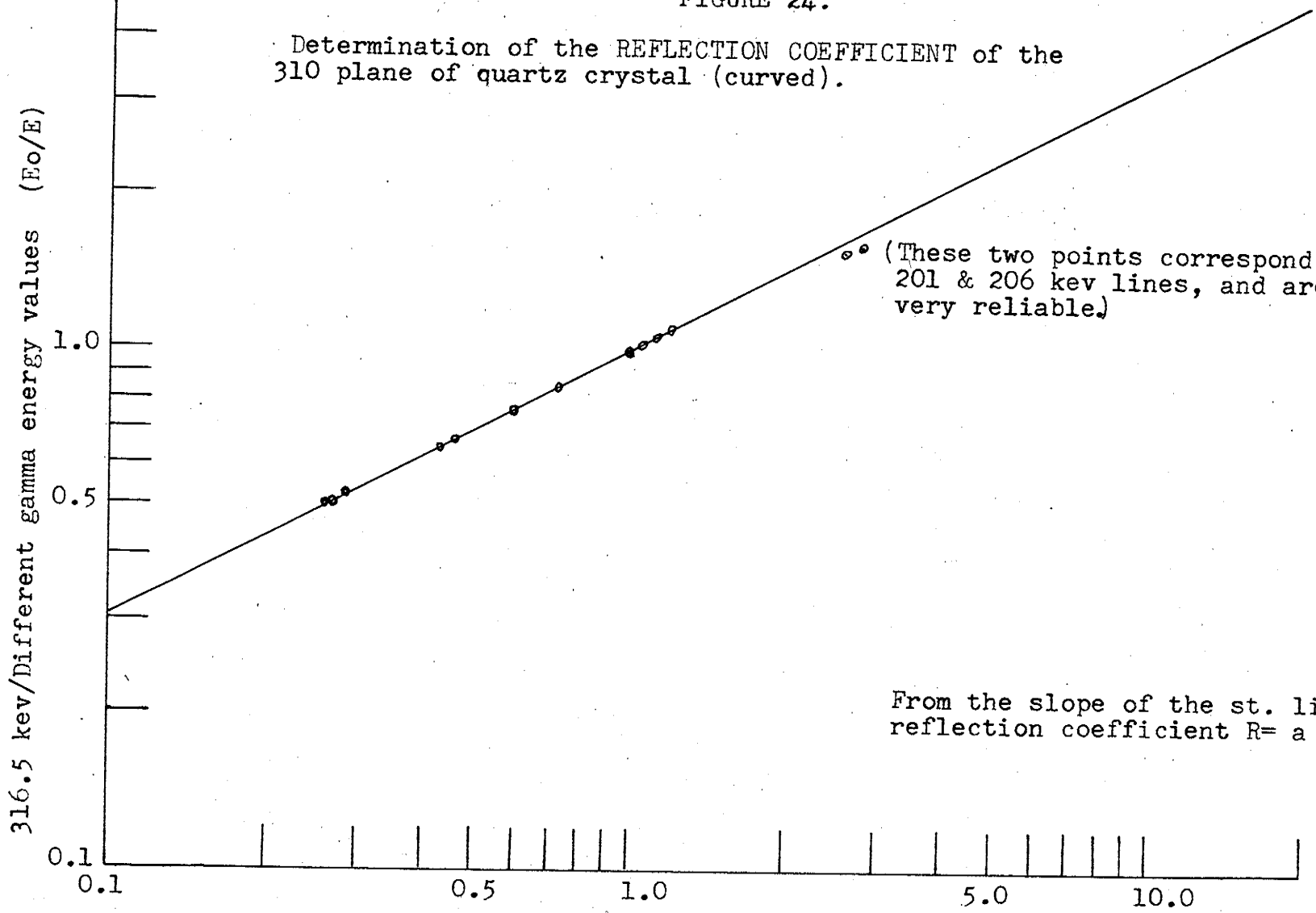

CHAPTER V

Determination of the reflection coefficient of the present crystal.

An attempt has been made to determine the reflectivity of the present crystal. The uncorrected intensity, Iu, (i.e. the photopeak area Ap) was corrected for self absorption, scintillation efficiency and photopeak efficiency (Fp), but not for reflectivity of the curved crystal. These values (IRu) are given in column 4 of table IX. These values (IRu) were divided by the respective relative intensities obtained with the help of the efficiency rule (i.e. by the respective values in column 1 of table IX). The ratios are given in column 4 of the same table. These ratios were plotted against respective Eo/E values (table VIII) on a log-log graph paper, and best fit straight line (which passes through more points) was drawn, again with the consideration that it should pass through (1,1) point (figure 24). From a knowledge of the slope of the straight line, the reflection coefficient R is found to be equal to : const. $E^{-1.95}$, within the energy range of 200 to about 600 kev. The present relation is pretty close to the relations given by Bergvall[26] and Edward et al[22], which have been mentioned earlier.

From the above mentioned graph (figure 24) it can be seen that, the straight line passes through almost all the points, but not through the representative points of 201 and 206 kev lines. This is possibly due to the fact that values for these lines in column 3 of table IX are not correct, as Fp values for these two lines are not known correctly.

Determination of the energy resolution of the diffraction spectrometer.

Energy resolution of the present 1.2 meter curved crystal diffraction spectrometer has been determined. Values of full width at half

TABLE X

Energy Resolution of the Present Spectrometer

Spectral energy line in kev unit	Resolution
E	$\frac{\Delta E}{E}$ (per cent)
136.3	0.25 ± 0.05
201.3	0.36 ± 0.02
205.8	0.29 ± 0.01
283.3	0.48 ± 0.06
295.9	0.53 ± 0.01
308.5	0.59 ± 0.02
316.5	0.59 ± 0.01
374.6	0.63 ± 0.04
416.6	0.75 ± 0.07
468.0	0.82 ± 0.02
484.6	0.89 ± 0.05
588.9	1.03 ± 0.05
604.7	1.04 ± 0.05
612.9	0.97 ± 0.07

FIGURE 25.

Determination of the energy resolution (as a function of energy) of the 1.2 meter curved crystal gamma ray spectrometer.

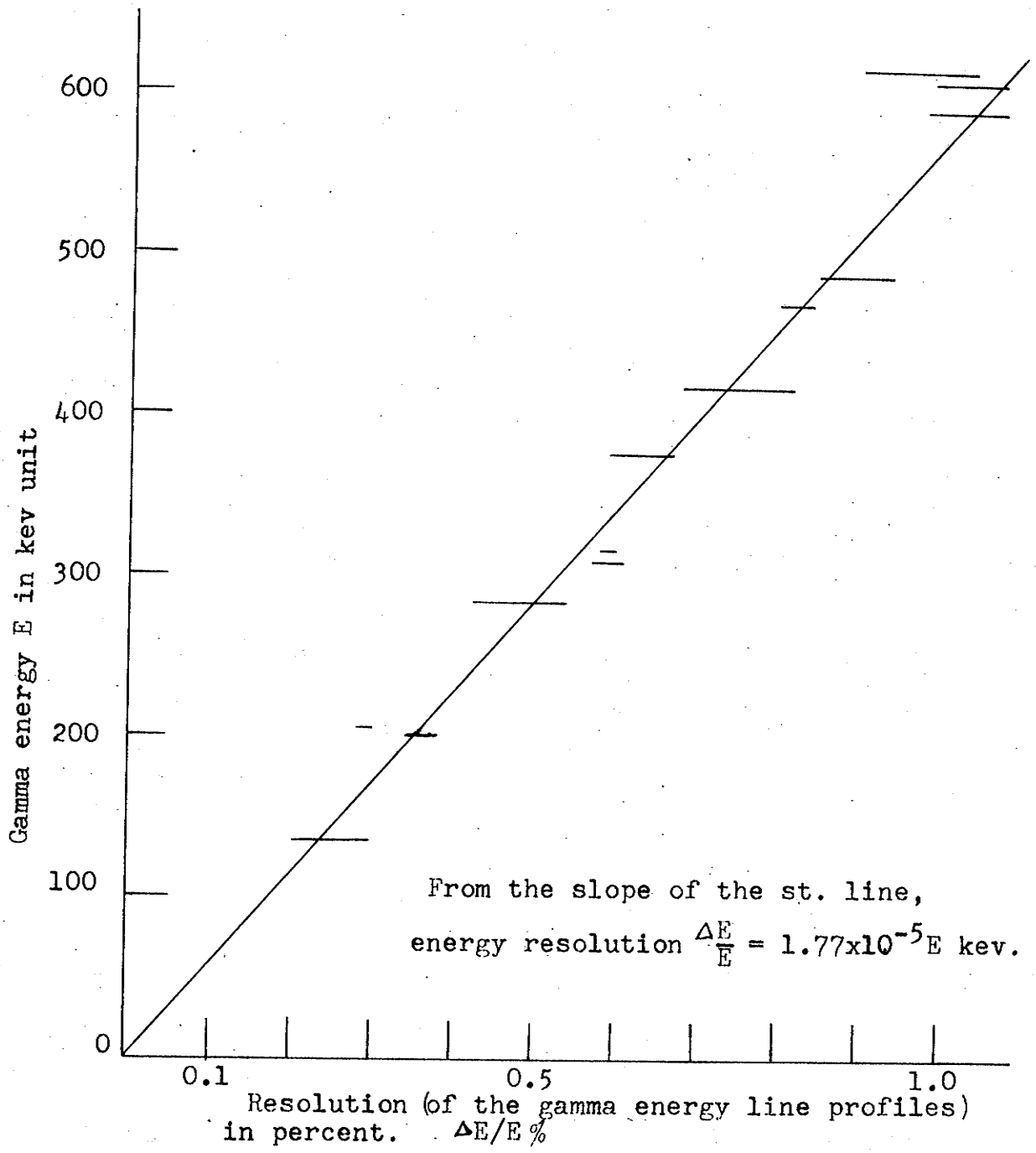

maximum divided by the line position for each photopeak (table X) were plotted against gamma energies of the respective lines (figure 25). The curve passing through all these points was a straight line. This straight line passes through the point (0,0). From the slope of this straight line energy resolution was determined as follows:

$$\frac{\Delta E}{E} = 1.77 \times 10^{-5} \text{ E (kev)}$$

within an upper limit of about 600 kev.

Edwards et al[22] have reported the energy resolution of the 2 meter curved crystal diffraction spectrometer at the California Institute of Technology as:

$$\frac{\Delta E}{E} = 2.3 \times 10^{-5} \text{ E (kev)}.$$

Lindstroem and Marklund[10] have reported the energy resolution of their 2 meter curved crystal diffraction spectrometer as

$$\frac{\Delta E}{E} = 1.4 \times 10^{-5} \text{ E (kev)}.$$

Search for other lines.

Lindstroem and Marklund[10] have reported relative intensities of three new lines as follows: 280 kev--- ≤ 1, 320 kev--- 15 ± 5, and 489 kev--- 4 ± 2 by photo conversion method. An attempt was made to investigate these transitions, without success. These transitions, if present, were indistinguishable from background. The reason may be as follows: Taking the values quoted by Lindstroem as correct, the line 280 kev is too weak to be observed, the line 320 kev may easily be obscured by the 316.5 kev line, strongest of all the transitions. The line 489 kev does not appear to be too weak and there is also no strong transition near its energy value. However, this transition could not be detected.

Huq[16] has reported the following additional transitions in Pt 192

45 kev, 96.8 kev, 104.7 kev, 156.7 kev, 167.5 kev, 400.9 kev and 437.4 kev; while Johns and Nablo[17] have reported the transitions 174 kev and 440 kev. A search was made for all these transitions, but the attempt has been unsuccessful. These lines also, if present, were indistinguishable from the background.

APPENDIX

Conversion of full width at half maximum readings (of a line profile) in number of dial turns into seconds of arc.

Changing wavelength into energy, the Bragg relation can be written as follows:

(1) $\lambda = \frac{hc}{E} = 2\ d \sin\theta$, for a first order spectrum.

Here h (Planck's constant) = 6.63×10^{-34} joule-sec.

c (speed of light) = 3.00×10^{8} meters/sec.

E, energy associated with the wavelength,

d (interplaner spacing of the 310 plane of quartz crystal = 1.1776 A°.)

and θ, the Bragg diffraction angle.

By substitution of the values of constants, the following relation can be obtained:

(2) $\sin\theta = \frac{5.26\ (kev)}{E\ (kev)}$, or, $E = \frac{5.26}{\sin\theta}$

From figure 1, $\sin\theta = \frac{R'B}{R'C}$.

R'B is proportional to the number of dial turns D and R'C is a constant.

(3) $\frac{hc}{E} = \lambda = 2\ d \sin\theta$, or, $E = \frac{hc}{2\ d \sin\theta} = \frac{K}{D}$, where K is a constant and D, number of dial turns (i.e. dial reading).

So, $E = \frac{K}{D} = \frac{5.26}{\sin\theta}$ and $D = \frac{K}{5.26} \sin\theta$.

Differentiating, we get

$$\delta D = \frac{K}{5.26} \cos\theta \cdot \delta\theta .$$

or, $\delta\theta = \frac{D}{\frac{K}{5.26}\cos\theta}$ radians $= \frac{\delta D}{\frac{K}{5.26}\cos\theta} \times 206{,}265$ seconds of arc.

Values of θ (and hence $\cos\theta$) can be found from relation (2) for different energy lines.

So $\delta\theta$ in seconds of arc for each line profile can easily be calculated, if δD, the number of dial turn for full width at half maximum is known.

For the investigated energy range reported in this thesis, the relation has been found (by calculation) to be linear. The relation is:

$$\delta\theta = 150.8 \times \delta D \text{ seconds of arc.}$$

LIST OF REFERENCES

1) Rutherford and Andrade, Phil. Mag. 27 (1914) 854, 28 (1914) 263

2) Bragg, W. H. and Bragg, W. L., Proc. Roy. Soc. A 88 (1913) 428

3) Thibaud, C. R. Acad. Sci. Paris 180 (1925) 138

4) Frilley, Ann. Phys. 11 (1929) 483

5) DuMond and Kirpatrick, Rev. Sci. Instrum. 1 (1930) 88

6) Cauchois, C. R. Acad. Sci. Paris 194 (1932) 362

7) DuMond, The Spectroscopy of Nuclear Gamma Rays by
Direct Crystal Diffraction Methods;
Published by California Institute of Technology,
Pasadena, California, March, 1954

8) DuMond, Rev. Sci. Instr. 18 (1947) 626

9) Goldhaber and Keown, Phys. Rev. Lett. 3 (1959) 47

10) Lindstroem and Marklund, Nucl. Phy. 49 (1963) 609

11) Muller et al, Phys. Rev. 88 (1952) 775

12) Baggerly et al, Phys. Rev. 100 (1955) 1364

13) Ryde and Anderson, Proc. Phys. Soc. B, 68 (1954) 1117

14) Sumbaev, Soviet Physics (J.E.T.P.) 5 (1957) 170

15) Kelman et al, Nucl. Phy. 4 (1957) 240

16) Huq, II Nuovo Cimento 5 (1957) 1456

17) Johns and Nablo, Phys. Rev. 96 (1954) 1599

18) Mraz, Nuclear Physics 4 (1957) 457

19) Kelly and Wiedenbeck, Phys. Rev. 102 (1956) 1130

20) Hamilton et al, Arkiv för Fysik 22 (1962) 485

21) Marklund and Lindstroem, Nucl. Phy. 40 (1963) 329

22) Edward et al, Nucl. Phy. 26 (1961) 670

23) John F. Moore, M.Sc. Thesis (1959), University of Manitoba

24) J. B. Birks, Theory and Practice of Scintillation Counting, Pergamon Press (1964)

25) Mott and Sutton, Handbuch Der Physik XLV (1958)

26) Bergvall, Arkiv för Fysik 17 (1960) 125

27) Hultberg, Arkiv för Fysik 15 (1959) 307

28) Frey et al, Arkiv för Fysik 21 (1962) 383

29) Lind et al, Phys. Rev. 77 (1950) 475

30) Alpha, Beta and Gamma-ray Spectroscopy, Volume 1, Edited by-Kai Siegbahn, North-Holland Publishing Company (1965)